EUROPEAN JOURNAL OF PURE AND APPLIED MATHEMATICS
2025, Vol. 18, Issue 2, Article Number 5861
ISSN 1307-5543 – ejpam.com
Published by New York Business Global

A Mathematical Model of COVID-19 Using Piecewise Derivative of Fractional Order

Shabana Naz[1], Muhammad Sarwar[1,2], Kamal Shah[1,2], Nahid Fatima[2], Thabet Abdeljawad[3,2,4,*]

[1] *Department of Mathematics, University of Malakand, Chakdara Dir(L), 18000, Khyber Pakhtunkhwa, Pakistan*
[2] *Department of Mathematics and Sciences, Prince Sultan University, Riyadh, 11586, Saudi Arabia*
[3] *Department of Mathematics, Saveetha School of Engineering, Saveetha Institute of Medical and Technical Sciences, Saveetha University, Chennai 602105, Tamil Nadu, India*
[4] *Department of Mathematics and Applied Mathematics, School of Science and Technology, Sefako Makgatho Health Sciences University, Ga-Rankuwa, South Africa*

Abstract. Currently the dynamical systems of infectious disease were studied by using various definitions of fractional calculus. Because the mentioned area has the ability to demonstrate the short and long memory terms involved in the physical dynamics of numerous real world problems. In this work, we consider a seven compartmental model for the transmission dynamics of COVID-19 including susceptible (S), vaccinated (V), exposed (E), infected (I), quarantined (Q), recovered (R), and death (D) classes. We first revisit the fundamental outcomes related to equilibrium points, basic reproduction numbers, sensitivity analysis, and equilibrium points including disease free (DF) and endemic equilibrium (EE) points. In addition, our main goal is to investigate the considered model under the new aspect of fractional calculus known as piecewise fractional order operators. The mentioned operators have the ability to demonstrate the multi phase behaviours of the dynamical problems. The said characteristics cannot be described by using the traditional operators. We apply the tools of nonlinear analysis to deduce sufficient conditions for the existence of at least one solution and its uniqueness. Additionally, we also investigate the results related to stability analysis of Ulam-Hyers (UH) type. Finally, we extend the concepts of RK2 method to form a sophisticated algorithm to simulate the results graphically. We present the numerical results for various fractional orders.

2020 Mathematics Subject Classifications: 26A33, 34A08, 03C65

Key Words and Phrases: Crossover effect, Fractional calculus, Stability, Numerical Results, Sensitivity

*Corresponding author.
DOI: https://doi.org/10.29020/nybg.ejpam.v18i2.5861

Email addresses: sarwarswati@gmail.com (M.Sarwar), kamalshah408@gmail.com kshah@psu.edu.sa (K. Shah), nfatima@psu.edu.sa (N. Fatima),tabdeljawad@psu.edu.sa (T. Abdeljawad)

1. Introduction

Mathematical models constitutes an interesting and applicable area of research to describe various real world problems. The said concept was initiated Bernoulli in 1776. Later on the idea was formally presented by Karmark and his co-authors in 1927 who established a simple susceptible infected and recovered (SIR) type model [13]. In subsequent years the mentioned area was increasingly extended to model various real world problems mathematically [10]. It is authenticating that epidemiology is the important area of medical field. Therefore, researchers have increasingly used mathematical models of classical, or difference type differential equations for mathematical models of various infectious diseases [11, 16]. Since infectious diseases have been investigated by using the idea of mathematical models. Researchers in majority of published work have used ordinary derivatives or simple algebraic type equations [19] to study the mentioned area. One of the major infectious diseases is caused by coronavirus known as severe acute respiratory syndrome coronavirus 2 (SARs-COV-2). Recently the said infectious disease gave birth a world wide pandemic in which more than 6 millions people have died. Also more than 60 millions have infected . Still the disease is in progress around the globe [44] . In the end of 2019, the first patient was reported in Wuhan China. Then many cases were reported in the coming few months. At the end of March there were 11 millions people been infected in the Wuhan city in which nearly 4 thousands were died. In April 2020 the said diseases were spread in many countries of the world and hence WHO announced it a global outbreak [47]. Many countries of the globe implemented lockdown and imposed strict precautionary measures to control the disease from further spreading. In the mean time, researchers of medical and bio-engineering fields focused on investigating the cure or proper medicine for the diseases [6].

Here, we remark that researchers of bio-engineering and applied sciences developed various mathematical models to investigate the transmission dynamics of the mentioned diseases [18]. Researchers used classical calculus and algebraic tools to investigate the said infectious disease. They used traditional tools for numerical simulations in their models. For instance authors [29] studied the following compartmental model of SARS-COV-2

using integer order derivative as follows:

$$\begin{cases} \frac{d}{dt}[S(t)] = \Lambda - \Big[b(1-p\xi)I(t) + (\eta + d)\Big]S(t), \\ \frac{d}{dt}[V(t)] = \eta S(t) - \Big[wbI(t) + d\Big]V(t), \\ \frac{d}{dt}[E(t)] = wbV(t)I(t) + b(1-p\xi)S(t)I(t) - (\tau + d)E(t), \\ \frac{d}{dt}[I(t)] = \tau E(t) - (\alpha_I + \delta_I + \sigma_I + d)I(t), \\ \frac{d}{dt}[Q(t)] = \alpha_I I(t) - [\sigma_Q + \delta_Q + d]Q(t), \\ \frac{d}{dt}[R(t)] = \sigma_I I(t) + \sigma_Q Q(t) - dR(t), \\ \frac{d}{dt}[D(t)] = \delta_I I(t) + \delta_Q Q(t), \\ \quad S(0) = S_0,\ V(0) = V_0,\ E(0) = E_0,\ I(0) = I_0,\ Q(0) = Q_0, \\ \quad R(0) = R_0,\ D(0) = D_0. \end{cases} \tag{1}$$

The nomenclatures are described as: Λ is denoted birth or recruitment rate, b stands for transmission rate of infection, p for rate of individuals who wear face masks, ξ is used for the rate of effectiveness of face masks, α_I stands for the rate of isolation of infected people. In addition, σ_I denoted recovered people rate, δ_I denotes mortality rate of infection, σ_Q denotes recovered people during isolation, δ_Q represents death rate of quarantined people due to infection. Further, d stands for natural death rate, and w stands for the rate of reduction due to vaccination process, η denotes rate of vaccination, and τ stands for incubation period.

On the other hand due to the significant use of fractional calculus in mathematical models of real world problems, researchers have introduced many operators for integrations and differentiations with real and complex orders. Since traditional tools of calculus cannot describe the past history and memory terms involved in the mathematical models of real world problems. Also, most of the biological populations dynamical systems consist of discrete type quantities which cannot be understood using ordinary derivatives and integrals. Therefore, researchers recommend for better understanding the dynamical behavior of real world problems by using the techniques of fractional calculus [15]. Some valuable work recently conducted on the aforementioned area, we refer to [5, 25, 26, 32, 37]. For the importance of mathematical models, we refer to [28].

After looking at the existing literature, we found that numerous mathematical models have been developed to examine the illness of SARS-COV-2 using different concepts of fractional orders derivatives. As a result, a great deal of research has been done on these pandemic using compartmental models with vaccinated class. However, after a careful examination, we noted that the mathematical models of the said disease with seven compartments have not been adequately examined in relation to the piecewise derivatives to

investigate the multi-phase dynamics. Therefore, in this regard, we need further investigation of such models to develop the computational as well as theoretical results for better understanding. As of October 10, 2020, the novel coronavirus, known as COVID-19, had spread to more than 200 nations globally and resulted in over 36 million confirmed cases. As a result, a number of machine learning models that can predict the outbreak worldwide have been made public. Researchers have developed huge amount of research work about the said diseases by using the concepts of mathematical models. Compartmental models have played great roles in predicting the future dynamics of such infectious diseases. Infectious diseases were regularly investigated by researchers by using various tools of mathematics. We refer some remarkable work as [22, 31, 35, 41, 48]. The mentioned area has been greatly applied in various disciplines to study various real world problems. Because it has many important applications. We refer to some [23, 27, 42, 48]. But fractional derivatives have not been uniquely defined yet. There are several approaches which are used by researchers. Recently, researchers found that some evolution processes suffer from abrupt changes in their state of dynamics. In such effect the process starts to show multi phase behaviours which cannot be explained by traditional calculus or fractional calculus concepts. Therefore, Atangana and his co-author [8] used piecewise concepts and brilliantly deduced some remarkable results for various dynamical problems. Some contribution of piecewise derivatives, we offer here as [20, 21, 45].

Many real world problems exhibit abrupt changes in their state of dynamics. For example earth quake, fluctuation in economy of less developed countries, and propagations of infections in society [46]. The mentioned sudden or abrupt changes in the dynamics of real world problems cannot be accommodate by using the classical tools of calculus. For these purposes recently researchers [7] introduced the concept of piecewise derivatives of fractional orders. The mentioned concepts were applied in many real world problems investigations using mathematical models. Researchers found that the said area excellently accommodate the concerned gap and comprehensively explain the dynamics of those evolution processes preserving the crossover or multi-phase dynamics [36]. The mentioned tools have not been yet applied in the mathematical model of SARS-COV-2 given in (1) to investigate the crossover dynamics. To fill this gap and to investigate the crossover dynamics of the model under the piecewise derivative concepts, we will follow the theory given in [40] and numerical procedures to achieve our study. Also, for numerical tools and qualitative analysis we utilized the procedures given in [9, 30, 38].

Hence inspired from the useful applications of piecewise derivatives of fractional order, we will extend the seven compartmental model given in (1) under the piecewise derivative of fractional order for further study in this project. We will establish the qualitative theory of existence of solution by using fixed point theory of Banach and Schauder type. Additionally, we will study the global stability under the mentioned piecewise derivative by using Volterra-Laypunov method. We also establish a numerical scheme based on the modified Euler method to simulate our theoretical results graphically. Here, we state that the local stability around the best numerical solution for any solution of the considered model (1) will be studied by using UH concept. To achieve the above statements, our

proposed model will be described as follows:

$$\begin{cases} {}_0^{\mathcal{PC}}D_t^{\varepsilon}[S(t)] = \Lambda - \Big[b(1-p\xi)I(t) + (\eta+d)\Big]S(t), \\ {}_0^{\mathcal{PC}}D_t^{\varepsilon}[V(t)] = \eta S(t) - \Big[wbI(t) + d\Big]V(t), \\ {}_0^{\mathcal{PC}}D_t^{\varepsilon}[E(t)] = wbV(t)I(t) + b(1-p\xi)S(t)I(t) - (\tau+d)E(t), \\ {}_0^{\mathcal{PC}}D_t^{\varepsilon}[I(t)] = \tau E(t) - (\alpha_I + \delta_I + \sigma_I + d)I(t), \\ {}_0^{\mathcal{PC}}D_t^{\varepsilon}[Q(t)] = \alpha_I I(t) - [\sigma_Q + \delta_Q + d]Q(t), \\ {}_0^{\mathcal{PC}}D_t^{\varepsilon}[R(t)] = \sigma_I I(t) + \sigma_Q Q(t) - dR(t), \\ {}_0^{\mathcal{PC}}D_t^{\varepsilon}[D(t)] = \delta_I I(t) + \delta_Q Q(t), \end{cases} \tag{2}$$

where ${}_0^{\mathcal{PC}}D_t^{\varepsilon}$ denotes piecewise derivative with fractional order $\varepsilon \in (0,1]$. Here, we investigate the model over $[0,\mathrm{T}]$ which can be expressed in sub intervals described by $\nabla_1 = [0,t_1],\ \nabla_2 = (t_1,\mathrm{T}]$. The flow chart of the model is given in figure 1.

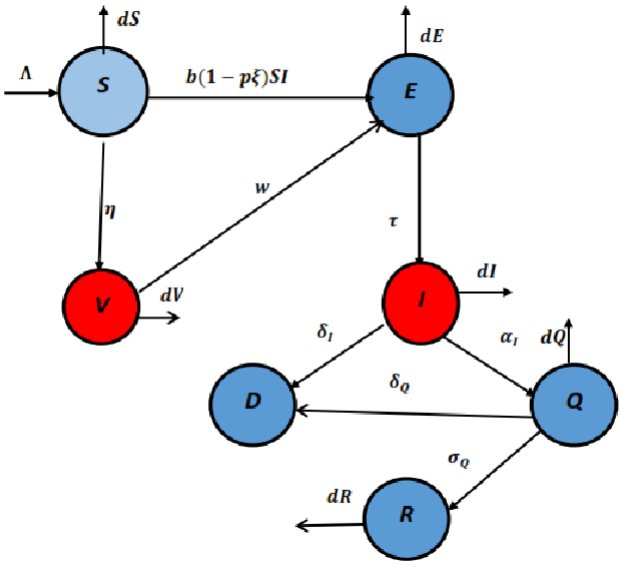

Figure 1: Flow chart of model (2).

In addition, the involve parameters have been described with their numerical values as in table 1

Nomenclatures	Description	Values
Λ	Natural birth rate	0.0020
b	Infection transmission rate	0.00005
p	The proportional of facing mask	0.01
ξ	The rate of efficacy of face masks	0.01
η	Rate of vaccination	0.02202643
τ	Period of incubation	0.05
d	Natural martially rate	0.019
ω	Recovery rate	0.0099259
α_I	Isolation rate of infected people	0.020
δ_I	The rate at which infected die	0.010
σ_I	The rate at which infected recovered	0.10
σ_Q	The rate at which quarantine recovered	0.013978
δ_Q	The rate at which quarantine die	0.015

Table 1: Nomenclature, description and values.

In our study, we also compute the feasible region, positivity and boundedness of solution under the mentioned derivative and equilibrium points. Also, the basic reproductive numbers together with the equilibrium points will be deduced for the model (2). Also an attempt will be done to investigate the sensitivity analysis of the basic reproduction number by following [34]. Results related to global stability of endemic equilibrium have been studied by using Volterra-Lyapunov method [43]. Some results devoted to existence theory and Ulam stability have been investigated by using tools used in [1, 14, 17] and [12, 33, 39]. The numerical investigations are investigated by establishing a numerical scheme based on the procedure given in [24]. Finally the results for various fractional orders will be presented graphically. Various models of dynamical systems like studied in [2–4], researchers have used fractional derivatives with power law type kernels to investigate the numerical solutions. Our study uses piecewise version of fractional derivative to investigate the existence and numerical solution for seven compartmental models.

2. Fundamental Results

Here, we recall some basic definitions from fractional calculus. For the given definitions we have used [32].

Definition 1. *The ML function is a recognisee generalization of the exponential. The ML function with one argument is defined as follows:*

$$\mathbf{E}_{\varepsilon}(t) = \sum_{k=0}^{\infty} \frac{t^k}{\Gamma(k\varepsilon + 1)},$$

while for double parameters it is defined as described by:

$$\mathbf{E}_{p,q}(t) = \sum_{k=0}^{\infty} \frac{t^k}{\Gamma(kp+q)}.$$

Definition 2. *[5] The Riemann-Liouville (RL) fractional integral with fractional order $\varepsilon > 0$ for a continuous function ϕ on $[0, \mathrm{T}]$ is defined by*

$$I_{0+}^{\varepsilon}\phi(t) = \frac{1}{\Gamma(\varepsilon)} \int_0^t (t-\varphi)^{\varepsilon-1}\phi(\varphi)d\varphi, \tag{3}$$

such that integral exists on right side.

Definition 3. *[5] The RL differentiation with non-integer order $n-1 < \varepsilon < n$ of a function ϕ which has absolutely continuous derivative up $(n-1)$ is defined by*

$$D_{0+}^{\varepsilon}\phi(t) = \frac{1}{\Gamma(n-\varepsilon)} \left(\frac{d}{dt}\right)^n \int_0^t (t-\varphi)^{n-\varepsilon-1}\phi(\varphi)d\varphi,$$

where $n = [\varepsilon] + 1$.

Definition 4. *[26] The Caputo fractional order derivative of order $n-1 < \varepsilon < n$ of a differentiable function $\phi \in C^n[0, \mathrm{T}]$ is defined by*

$${}^{C}D_{0+}^{\varepsilon}\phi(t) = \frac{1}{\Gamma(n-\varepsilon)} \int_0^t (t-\varphi)^{n-\varepsilon-1}\phi^{(n)}(\varphi)d\varphi,$$

where $n = [\varepsilon] + 1$.

Lemma 1. *[26]The given equation*

$$\begin{aligned} &{}^{C}D_{0+}^{\varepsilon}\phi(t) = \chi(t), \\ &\phi(0) = \phi_0 \end{aligned} \tag{4}$$

has a solution of the form

$$\phi(t) = \phi_0 + \frac{1}{\Gamma(\varepsilon)} \int_0^t (t-\varphi)^{\varepsilon-1}\chi(\varphi)d\varphi. \tag{5}$$

Definition 5. *The piecewise integration of a continuous function ϕ such that $0 < t_1 < t_2 < t_3 < t$ is defined by*

$$\int_{t_1}^{t_3} \phi(t)dt = \int_{t_1}^{t_2} \phi(t)dt + \int_{t_2}^{t_3} \phi(t)dt.$$

Definition 6. *[37] The piecewise RL fractional integral of order $\varepsilon \in (0, 1]$ of a continuous function ϕ is described as*

$${}^{PRL}I_{0^+}^{\varepsilon}\phi(t) = \begin{cases} \displaystyle\int_0^{t_1} \phi(t)dt, \quad \textit{with} \ \ t \in \nabla_1, \\ \displaystyle\frac{1}{\Gamma(\varepsilon)} \int_{t_1}^{t} (t-\varphi)^{\varepsilon-1}\phi(\varphi)d\varphi, \quad \textit{with} \ \ t \in \nabla_2. \end{cases}$$

Definition 7. *[37] The piece-wise derivative of order $\varepsilon \in (0,1]$ in the Caputo sense of a differentiable function $\phi \in \mathrm{C}[0,T]$ is defined by*

$$ {}_0^{PC}D_t^{\varepsilon}\phi(t) = \begin{cases} \dfrac{d\phi(t)}{dt}, & with \;\; t \in \nabla_1, \\ {}^{C}D_{0+}^{\varepsilon}\phi(t), & with \;\; t \in \nabla_2, \end{cases} $$

such that ${}^{PC}D_{0+}^{\varepsilon}$ represents ordinary differentiation in ∇_1 and the Caputo differentiation on ∇_2.

Lemma 2. *[25] The solution of the problem*

$$ \begin{aligned} {}_0^{PC}D_t^{\varepsilon}\phi(t) &= \chi(t), \\ \phi(0) &= \phi_0, \end{aligned} $$

is given by

$$ \phi(t) = \begin{cases} \phi_0 + \displaystyle\int_0^{t_1} \chi(\varphi)d\varphi, & with \;\; t \in \nabla_1, \\ \phi(t_1) + \dfrac{1}{\Gamma(\varepsilon)} \displaystyle\int_{t_1}^{t} (t-\varphi)^{\varepsilon-1}\chi(\varphi)d\varphi, & with \;\; t \in \nabla_2. \end{cases} $$

Theorem 1. *[14]Let $D \subset \mathbf{B}$ be closed convex bounded set such that $D = \{z \in \mathbf{B} \; z = \lambda N z, \; \lambda \in [0,1]\}$,, then $N : D \to \mathbf{B}$ is completely continuous operator has at least one fixed point.*

Definition 8. *According to Ulam [12, 33, 39] "near every exact function there are many approximation of it". According to their definition consider a functional equation given by*

$$ Nz = z $$

is UH stable if for any $\varepsilon > 0$, for the inequality

$$ |z - Nz| \leq \varepsilon, \;\; z \in \mathbf{B}, $$

and constant $L_N > 0$ one has

$$ |z - z^*| \leq L_N \varepsilon, $$

where z^* is the best approximate or exact solution.

Definition 9. ***Sensitivity index****[34]*
It is an important threshold value calculated by the formula given by

$$ \mathbf{S}_p^{\mathcal{R}_0} = \frac{p}{\mathcal{R}_0}\frac{\partial \mathcal{R}_0}{\partial p}, \tag{6} $$

were p is the parameter describing the relation of $\mathcal{R}_0$. Sensitivity index tells us how much be the dynamic effected by increasing or decreasing the values of parameters.

3. Fundamental Results of Model (2)

Here we provide the positivity, boundedness, DF and EE points. Also we compute the basic reproductive number and presents its 3D profile. Sensitivity is also discussed here.

Theorem 2. *All solutions of model* (2) *are bounded and inclined to a feasible region described by*

$$\Omega = \left\{ (S,V,E,I,Q,R) \in \mathbb{R}^6_+ S+V+E+I+Q+R \leq \frac{\Lambda}{d} \right\}.$$

Proof. Let M be the total pollution at time $t>0$, such that

$$M(t) = S(t)+V(t)+E(t)+I(t)+Q(t)+R(t). \tag{7}$$

Applying ${}^{\mathcal{PC}}_{0}D^{\varepsilon}_{t}$ to both sides of (7) gives

$$\begin{aligned} {}^{\mathcal{PC}}_{0}D^{\varepsilon}_{t}[M(t)] &= {}^{\mathcal{PC}}_{0}D^{\varepsilon}_{t}[S(t)] + {}^{\mathcal{PC}}_{0}D^{\varepsilon}_{t}[V(t)] + {}^{\mathcal{PC}}_{0}D^{\varepsilon}_{t}[E(t)] + {}^{\mathcal{PC}}_{0}D^{\varepsilon}_{t}[I(t)] \\ &+ {}^{\mathcal{PC}}_{0}D^{\varepsilon}_{t}[Q(t)] + {}^{\mathcal{PC}}_{0}D^{\varepsilon}_{t}[R(t)]. \end{aligned} \tag{8}$$

Using the corresponding values from (2) in (7) and simplifying, we get

$$\begin{aligned} {}^{\mathcal{PC}}_{0}D^{\varepsilon}_{t}[M(t)] &= \Lambda - d(S+E+V+I+Q+R) \\ &= \Lambda - dM. \end{aligned} \tag{9}$$

We can write (9)

$${}^{\mathcal{PC}}_{0}D^{\varepsilon}_{t}[M(t)] = \begin{array}{l} \frac{dM}{dt} = \Lambda - dM,\ t \in \nabla_1, \\ {}^{\mathcal{C}}_{0}D^{\varepsilon}_{t}[M(t)] = \Lambda - dM,\ t \in \nabla_2. \end{array} \tag{10}$$

Applying Laplace transform in (15) yields that

$$M(t) = \begin{array}{l} \frac{\Lambda}{d} - M_0 \exp(-dt),\ t \in \nabla_1, \\ \frac{\Lambda}{d}\left(1 - \mathbf{E}_{\varepsilon}(-dt^{\varepsilon})\right) + \mathbf{E}_{\varepsilon}(-dt^{\varepsilon}),\ t \in \nabla_2. \end{array} \tag{11}$$

Hence at $t \to \infty$, we get from (11)

$$M(t) \leq \frac{\Lambda}{d}.$$

Theorem 3. *All the solutions* (S,V,E,I,Q,R,D) *of model* (2) *are non-negative for* $t>0$ *with positive initial condition* $(S_0,V_0,E_0,I_0,Q_0,R_0,D_0)>0$.

Proof. From model (2), we have

$$\begin{aligned}
{}_0^{\mathcal{PC}}D_t^{\varepsilon}[S(t)]\Big|_{S=0} &= \Lambda > 0,\\
{}_0^{\mathcal{PC}}D_t^{\varepsilon}[V(t)]\Big|_{V=0} &= 0,\\
{}_0^{\mathcal{PC}}D_t^{\varepsilon}[E(t)]\Big|_{E=0} &= 0,\\
{}_0^{\mathcal{PC}}D_t^{\varepsilon}[I(t)]\Big|_{I=0} &= 0,\\
{}_0^{\mathcal{PC}}D_t^{\varepsilon}[Q(t)]\Big|_{Q=0} &= 0,\\
{}_0^{\mathcal{PC}}D_t^{\varepsilon}[R(t)]\Big|_{R=0} &= 0,\\
{}_0^{\mathcal{PC}}D_t^{\varepsilon}[D(t)]\Big|_{D=0} &= 0,
\end{aligned}$$

from (12), one see that ${}_0^{\mathcal{PC}}D_t^{\varepsilon}[S(t)] > 0$ which yields that $S(t) > 0$, at $t > 0$, hence we conclude that $(S, V, E, I, Q, R, D) > 0$ at $t > 0$. Hence positivity condition derived.

Further, the DFE and endemic equilibrium points can be computed by using the results of [29] as follows:

DFE

From (2) putting left sides equal to zeros, that is

$$\left.\begin{aligned}
\Lambda - \Big[b(1-p\xi)I(t) + (\eta + d)\Big]S(t) &= 0,\\
\eta S(t) - \Big[wbI(t) + d\Big]V(t) &= 0,\\
wbV(t)I(t) + b(1-p\xi)S(t)I(t) - (\tau + d)E(t) &= 0,\\
\tau E(t) - (\alpha_I + \delta_I + \sigma_I + d)I(t) &= 0,\\
\alpha_I I(t) - [\sigma_Q + \delta_Q + d]Q(t) &= 0,\\
\sigma_I I(t) + \sigma_Q Q(t) - dR(t) &= 0,\\
\delta_I I(t) + \delta_Q Q(t) &= 0.
\end{aligned}\right\}$$

Now $I = 0, E = 0, Q = 0, R = 0, D = 0$ due to absence of infection, and $S = S^0, V = V^0$, and solving system (12), we have

$$\mathcal{E}^0 = \left(\frac{\Lambda}{\eta + d}, \frac{\Lambda}{d(\eta + d)}, 0, 0, 0, 0, 0\right).$$

Endemic equilibrium point

In the same way, we can compute endemic equilibrium point $\mathcal{E}^* = \left(\tilde{S}, \tilde{V}, \tilde{E}, \tilde{I}, \tilde{Q}, \tilde{R}, \tilde{D}\right)$,

again from equating right sides of model (2) equal to zero as follows:

$$\left.\begin{aligned}
\Lambda - \left[b(1-p\xi)\tilde{I}(t) + (\eta+d)\right]\tilde{S}(t) = 0,\\
\eta\tilde{S}(t) - \left[wb\tilde{I}(t) + d\right]\tilde{V}(t) = 0,\\
wb\tilde{V}(t)\tilde{I}(t) + b(1-p\xi)\tilde{S}(t)\tilde{I}(t) - (\tau+d)\tilde{E}(t) = 0,\\
\tau\tilde{E}(t) - (\alpha_I + \delta_I + \sigma_I + d)\tilde{I}(t) = 0,\\
\alpha_I\tilde{I}(t) - [\sigma_Q + \delta_Q + d]\tilde{Q}(t) = 0,\\
\sigma_I\tilde{I}(t) + \sigma_Q\tilde{Q}(t) - d\tilde{R}(t) = 0,\\
\delta_I\tilde{I}(t) + \delta_Q\tilde{Q}(t) = 0.
\end{aligned}\right\}$$

On solving (12), we get

$$\begin{cases}
\tilde{S} = \dfrac{\Lambda}{b(1-p\xi)\tilde{I} + \eta + d},\\
\tilde{V} = \dfrac{\eta}{wb\tilde{I} + d}\left[\dfrac{\Lambda}{b(1-p\xi)\tilde{I} + \eta + d}\right],\\
\tilde{E} = \dfrac{1}{\theta + d}\left[\dfrac{\Lambda b(1-p\xi)}{b(1-p\xi)\tilde{I} + \eta + d} + \dfrac{wb\eta\Lambda}{b(1-p\xi)\tilde{I} + \eta + d}\right]\tilde{I},\\
\tilde{I} = \dfrac{\theta}{(\alpha_I + \delta_I + \sigma_I + d)}\left[\dfrac{1}{\theta + d}\left[\dfrac{\Lambda b(1-p\xi)}{b(1-p\xi)\tilde{I} + \eta + d} + \dfrac{wb\eta\Lambda}{b(1-p\xi)\tilde{I} + \eta + d}\right]\tilde{I}\right],\\
\tilde{Q} = \dfrac{\alpha_I\tilde{I}}{\sigma_Q + \delta_Q + d},\\
\tilde{R} = \dfrac{\sigma_I}{d}\tilde{I} + \dfrac{\sigma_Q}{d}\dfrac{\alpha_I\tilde{I}}{\sigma_Q + \delta_Q + d},\\
\tilde{Q} = 0.
\end{cases}$$

The basic reproductive number $\mathcal{R}_0$ has been computed for integer order model in [29], we recall it as follows:

$$\mathcal{R}_{vac} = \frac{\tau b(1-p\xi)\Lambda}{(\tau+d)(\alpha_I + \delta_I + \sigma_I + d)}\left[\frac{d+\omega}{d(\eta+d)}\right], \tag{12}$$

but if no vaccination, then $\omega = 0$, we get the fundamental reproductive number as follows:

$$\mathcal{R}_0 = \frac{\tau b(1-p\xi)\Lambda}{d(\tau+d)(\alpha_I + \delta_I + \sigma_I + d)}. \tag{13}$$

In figure 2, we describe surface plot of the reproductive numbers to see the behaviour on decreasing or increasing the parameters values.

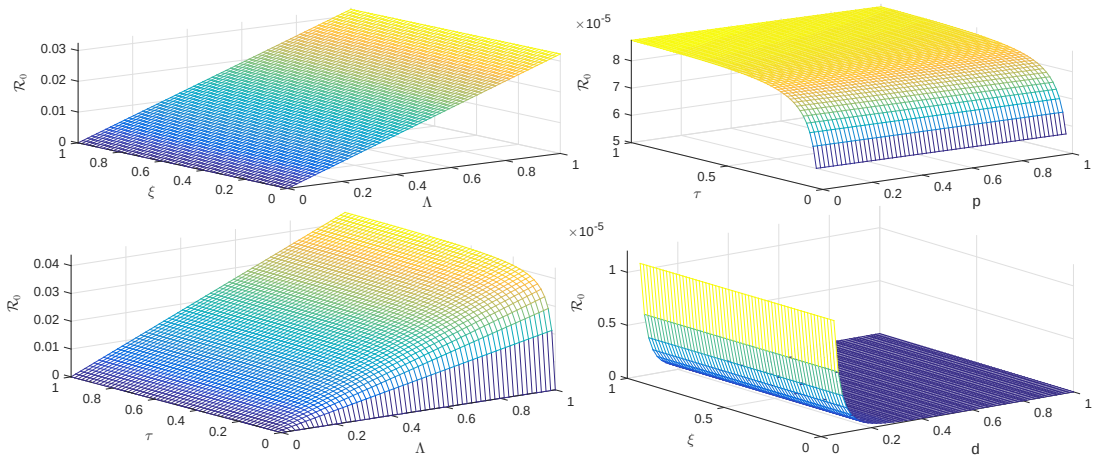

Figure 2: Surface plots of $\mathcal{R}_0$.

We see that as the values of the given parameters are decreasing, the value of $\mathcal{R}_0$ is also increasing but never exceeds 1.

3.1. Sensitivity Analysis

Next, we apply the formula to get the sensitivity of the fundamental reproduction number.

$$\mathbf{S}_q^{\mathcal{R}_0} = \frac{q}{\mathcal{R}_0}\frac{\partial \mathcal{R}_0}{\partial q}, \tag{14}$$

where q represents parameter involve in the $\mathcal{R}_0$. According to (14), we compute sensitivity indices 2.

Sensitivity index	Value	Sensitivity index	Value
$\mathbf{S}_b^{\mathcal{R}_0}$	1.0	$\mathbf{S}_\tau^{\mathcal{R}_0}$	1.0
$\mathbf{S}_\xi^{\mathcal{R}_0}$	- 0.637	$\mathbf{S}_d^{\mathcal{R}_0}$	-0.4567
$\mathbf{S}_p^{\mathcal{R}_0}$	-0.776	$\mathbf{S}_{\alpha_I}^{\mathcal{R}_0}$	-0.7675
$\mathbf{S}_\Lambda^{\mathcal{R}_0}$	1.0	$\mathbf{S}_{\delta_I}^{\mathcal{R}_0}$	-0.9986
$\mathbf{S}_{\sigma_I}^{\mathcal{R}_0}$	-0.895		

Table 2: Sensitivity indices of basic reproduction number.

From sensitivity indices table 2, we see that increase of specific percentage of values means that percentage increase or decrease in the index which implies the impact of parameters values for simulations in the current studies. Here, in figure 3, we present the pi chart of sensitivity indices which describe the percentage impact of variable on the reproductive number.

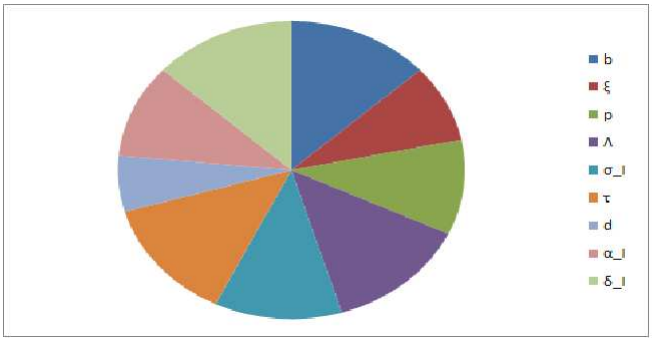

Figure 3: Plot of Sensitivity index.

4. Existence Theory

Let $\mathcal{J} = [0, \mathrm{T}],\ 0 \leq t \leq \mathrm{T} < \infty$, and $\phi = (S, V, E, I, Q, R, D)$, then the right sides of (2), we can express as

$$\begin{cases} \mathcal{L}_1(t, \phi(t)) = \Lambda - \Big[b(1 - p\xi)I(t) + (\eta + d)\Big]S(t), \\ \mathcal{L}_2(t, \phi(t)) = \eta S(t) - \Big[wbI(t) + d\Big]V(t), \\ \mathcal{L}_3(t, \phi(t)) = wbV(t)I(t) + b(1 - p\xi)S(t)I(t) - (\tau + d)E(t), \\ \mathcal{L}_4(t, \phi(t)) = \tau E(t) - (\varepsilon_I + \delta_I + \sigma_I + d)I(t), \\ \mathcal{L}_5(t, \phi(t)) = \varepsilon_I I(t) - [\sigma_Q + \delta_Q + d]Q(t), \\ \mathcal{L}_6(t, \phi(t)) = \sigma_I I(t) + \sigma_Q Q(t) - dR(t), \\ \mathcal{L}_7(t, \phi(t)) = \delta_I I(t) + \delta_Q Q(t). \end{cases} \tag{15}$$

Utilizing (15), model (2), with $\varepsilon \in (0, 1]$ may be express as:

$$\begin{cases} {}_0^{\mathcal{PC}}D_t^{\varepsilon}\phi(t) = \mathbf{g}(t, \phi(t)),\ t \in \mathcal{J}, \\ \phi(0) = \phi_0, \end{cases} \tag{16}$$

where

$$\phi(t) = \begin{cases} S(t), \\ V(t), \\ E(t), \\ I(t), \\ Q(t), \\ R(t), \\ D(t). \end{cases}, \quad \phi_0(t) = \begin{cases} S_0, \\ V_0, \\ E_0, \\ I_0, \\ Q_0, \\ R_0, \\ D_0. \end{cases} \quad \mathbf{g}(t, \phi(t)) = \begin{cases} \mathcal{L}_1(t, \phi(t)), \\ \mathcal{L}_2(t, \phi(t)), \\ \mathcal{L}_3(t, \phi(t)), \\ \mathcal{L}_4(t, \phi(t)), \\ \mathcal{L}_5(t, \phi(t)), \\ \mathcal{L}_6(t, \phi(t)). \end{cases} \tag{17}$$

Lemma 3. *For the function $g : [0, \mathrm{T} \times R \to R$, the given problem*

$$\begin{aligned} {}_0^{PC}\mathrm{D}_t^{\varepsilon}\phi(t) &= \mathbf{g}(t, \phi(t)), \quad 0 < \varepsilon \leq 1, \\ \phi(0) &= \phi_0 \end{aligned} \tag{18}$$

is equivalent to the integral equation described by

$$\phi(t) = \begin{cases} \phi_0 + \displaystyle\int_0^t \mathbf{g}(u, \phi(u))du, \ t \in \nabla_1, \\ \phi(t_1) + \displaystyle\int_{t_1}^{\mathrm{T}} \frac{(t-u)^{\varepsilon-1}}{\Gamma(\varepsilon)}\mathbf{g}(u, \phi(u))du, \quad t_1 < t \leq \mathrm{T}, \end{cases} \tag{19}$$

Proof. Following the fashion of Lemma 2, we can easily obtain the solution above.

The hypothesis given hold:

(H1) Let $\mathbf{L_g} > 0$ is real number and $\phi, \ \bar{\phi} \in \mathbf{B}$, then

$$|\mathbf{g}(t, \phi) - \mathbf{g}(t, \bar{\phi})| \leq \mathbf{L_g}|\phi - \bar{\phi}|.$$

(H2) Let $\mathbf{C_g} > 0$ and $\mathbf{M_g} > 0$, then

$$|\mathbf{g}(t, \phi(t))| \leq \mathbf{C_g}|\phi| + \mathbf{M_g}.$$

Theorem 4. *At least one solution exists for the Problem* (18) *under the hypotheses* $(H1), (H2)$.

Proof. Let define a closed and convex subset $\mathbf{D} \subset \mathbf{B}$ as

$$\mathbf{D} = \{\phi \in \mathbf{B} : \ \|\phi\| \leq \mathbf{r}_{1,2}, \ \mathbf{r}_{1,2} > 0\}.$$

Let $\mathbf{N} : \mathbf{D} \to \mathbf{D}$ using (35), then

$$\mathbf{N}(\phi) = \begin{cases} \phi_0 + \displaystyle\int_0^t \mathbf{g}(u, \phi(u))du, \quad t \in \nabla_1, \\ \phi(t_1) + \displaystyle\int_{t_1}^{\mathrm{T}} \frac{(t-u)^{\varepsilon-1}}{\Gamma(\varepsilon)}\mathbf{g}(u, \phi(u))du, \quad t_1 < t \leq \mathrm{T}. \end{cases} \tag{20}$$

For $\phi \in \mathbf{D}$, it follows that

$$|\mathbf{N}(\phi)(t)| \leq \begin{cases} |\phi_0| + \displaystyle\int_0^{t_1} |\mathbf{g}(u, \phi(u))|\mathrm{d}u, \\ |\phi(t_1)| + \displaystyle\int_{t_1}^{\mathrm{T}} \frac{(t-u)^{\varepsilon-1}}{\Gamma(\varepsilon)} |\mathbf{g}(u, \phi(u))| \, \mathrm{d}u \end{cases}$$

$$\leq \begin{cases} |\phi_0| + \int_0^{t_1} [\mathbf{C_g}\|\phi\| + \mathrm{M_g}]\, du, \\ |\phi(t_1)| + \int_{t_1}^{\mathrm{T}} \dfrac{(t-u)^{\varepsilon-1}}{\Gamma(\varepsilon)} [\mathbf{C_g}\|\phi\| + \mathrm{M_g}]\, du, \end{cases}$$

$$\leq \begin{cases} |\phi_0| + t_1 [\mathbf{C_g}\mathbf{r}_{1,2} + \mathbf{M_g}] \leq \mathbf{r}_{1,2}, \quad t \in \nabla_1, \\ |\phi(t_1)| + \dfrac{\mathrm{T}^{\varepsilon}}{\Gamma(\varepsilon+1)} [\mathbf{C_g}\mathbf{r}_{1,2} + \mathbf{M_g}] \leq \mathbf{r}_{1,2}, \ t_1 < t \leq \mathrm{T}, \end{cases}$$

for $t_1 < t \leq \mathrm{T}$, use $|(t_1-u)^{\varepsilon} - (\mathrm{T}-u)^{\varepsilon}| \leq \mathrm{T}^{\varepsilon}$, one has

$$\mathbf{r}_{1,2} \geq \max \begin{cases} \dfrac{|\phi_0| + t_1 \mathbf{M_g}}{1 - t_1 \mathbf{C_g}}, \ t \in \nabla_1, \\ \dfrac{|\phi(t_1)|\Gamma(\varepsilon+1) + \mathrm{T}^{\varepsilon}\mathbf{M_g}}{(\Gamma(\varepsilon+1) - \mathrm{T}^{\varepsilon}\mathbf{C_g}}, \ t_1 < t \leq \mathrm{T}. \end{cases}$$

Thus proved that $\|\mathbf{N}(\phi)\| \leq \mathbf{r}_{1,2}$, implies that $\mathbf{N}(\mathbf{D}) \subset \mathbf{D}$. Thus, bounded set to bounded set is mapped by $\mathbf{N}$. Hence, $\mathbf{N}$ is bounded. Take $t_{\mathrm{m}} < t_{\mathrm{n}} \in [0, t_1]$, we have

$$\begin{aligned} |\mathbf{N}(\phi)(t_{\mathrm{n}}) - \mathbf{N}(\phi)(t_{\mathrm{m}})| &= \left| \int_0^{t_{\mathrm{n}}} \mathbf{g}(u, \phi(u)) du - \int_0^{t_{\mathrm{m}}} \mathbf{g}(u, \phi(u)) du \right| \\ &\leq \int_{t_{\mathrm{m}}}^{t_{\mathrm{n}}} |\mathbf{g}(u, \phi(u))| du \\ &\leq \int_{t_{\mathrm{m}}}^{t_{\mathrm{n}}} [\mathbf{C_g}\|\phi\| + \mathbf{M_g}]\, du \\ &\leq (\mathbf{C_g}\mathbf{r}_{1,2} + \mathbf{M_g})[t_{\mathrm{n}} - t_{\mathrm{m}}]. \end{aligned} \tag{21}$$

The (21) tells us that $t_{\mathrm{m}} \to t_{\mathrm{n}}$, implies that

$$|\mathbf{N}(\phi)(t_{\mathrm{n}}) - \mathbf{N}(\phi)(t_{\mathrm{m}})| \to 0.$$

The uniform continuity of $\mathbf{N}$ implies that

$$\|\mathbf{N}(\phi)(t_{\mathrm{n}}) - \mathbf{N}(\phi)(t_{\mathrm{m}})\| \to 0, \text{ as } t_{\mathrm{n}} \to t_{\mathrm{m}}.$$

It follows that $\mathbf{N}$ is equi-continuous in this case.

Next, we take the other interval $t_{\mathrm{m}} < t_{\mathrm{n}} \in (t_1, \mathrm{T}]$ as

$$\begin{aligned} |\mathbf{N}(\phi)(t_{\mathrm{n}}) - \mathbf{N}(\phi)(t_{\mathrm{m}})| &= \left| \int_0^{t_{\mathrm{n}}} \frac{(t_{\mathrm{n}}-u)^{\varepsilon-1}}{\Gamma(\varepsilon)} \mathbf{g}(u, g(u)) du - \int_0^{t_{\mathrm{m}}} \frac{(t_{\mathrm{m}}-\tau)^{\varepsilon-1}}{\Gamma(\varepsilon)} \mathbf{g}(u, \phi(u)) du \right| \\ &\leq \int_0^{t_{\mathrm{m}}} \frac{[(t_m-u)^{\varepsilon-1} - (t_{\mathrm{n}}-u)^{\varepsilon-1}]}{\Gamma(\varepsilon)} |\mathbf{g}(u, \phi(u))| du \\ &+ \int_{t_{\mathrm{m}}}^{t_{\mathrm{n}}} \frac{(t_{\mathrm{n}}-u)^{\varepsilon-1}}{\Gamma(\varepsilon)} |\mathbf{g}(u, \phi(u))| du \end{aligned}$$

$$\begin{aligned} &\leq \left[\int_0^{t_{\mathrm{m}}} \frac{[(t_{\mathrm{m}}-u)^{\varepsilon-1}-(t_{\mathrm{n}}-u)^{\varepsilon-1}]}{\Gamma(\varepsilon)}du \right. \\ &+ \left. \int_{t_{\mathrm{m}}}^{t_{\mathrm{n}}} \frac{(t_{\mathrm{n}}-u)^{\varepsilon-1}}{\Gamma(\varepsilon)}du\right](\mathbf{C_g}\|\phi\|+\mathbf{M_g}) \\ &\leq \frac{(\mathbf{C_g}\mathbf{r}_{1,2}+\mathbf{M_g})}{\Gamma(\varepsilon+1)}\left[t_{\mathrm{n}}^{\varepsilon}-t_{\mathrm{m}}^{\varepsilon}+2(t_{\mathrm{n}}-t_{\mathrm{m}})^{\varepsilon}\right]. \end{aligned} \tag{22}$$

We see from (22), that

$$|\mathbf{N}(\phi)(t_{\mathrm{n}})-\mathbf{N}(\phi)(t_{\mathrm{m}})|\to 0,\ \text{as } t_{\mathrm{m}}\to t_{\mathrm{n}}.$$

As $\mathbf{N}$ is bounded over $[t_1,\mathrm{T}]$ and also uniformly continuous. Thus

$$\|\mathbf{N}(\phi)(t_{\mathrm{n}})-\mathbf{N}(\phi)(t_{\mathrm{m}})\|\to 0,\ \text{as } t_{\mathrm{m}}\to t_{\mathrm{n}}.$$

Hence, $\mathbf{N}$ is equi-continuous over $(t_1,\mathrm{T}]$.

Therefore, $\mathbf{N}$ is equi- continuous mapping over $[0,t_1]\cup(t_1,\mathrm{T}]$. By Arzelá-Ascoli theorem, $\mathbf{N}$ is completely continuous. Thus in view of Theorem 1, the problem (18) has at least one solution.

Theorem 5. *Under the hypothesis* $(H1)$*, the problem* (18) *has a unique solution with*

$$\max\left\{t_1\mathbf{L_g},\ \frac{\mathrm{T}^{\varepsilon}}{\Gamma(\varepsilon+1)}\mathbf{L_g}\right\}=\Delta<1$$

holds.

Proof. Let $\mathbf{N}:\mathbf{B}\to\mathbf{B}$ be the mapping, then for $\phi,\ \bar{\phi}\in\mathbf{B}$, we consider for $[0,t_1]$ as

$$\begin{aligned} \|\mathbf{N}(\phi)-\mathbf{N}(\bar{\phi})\| &= \max_{t\in[0,t_1]}\left|\int_0^{t_1}\mathbf{g}(u,\phi(u))du-\int_0^{t_1}\mathbf{g}(u,\bar{\phi}(u))du\right| \\ &\leq t_1\mathbf{L_g}\|\phi-\bar{\phi}\|. \end{aligned} \tag{23}$$

Hence , we have from (23)

$$\|\mathbf{N}(\phi)-\mathbf{N}(\bar{\phi})\|\leq t_1\mathbf{L_g}\|\phi-\bar{\phi}\|. \tag{24}$$

If $t_1\leq t\leq \mathrm{T}$, one has

$$\begin{aligned} \|\mathbf{N}(\phi)-\mathbf{N}(\bar{\phi})\| &= \max_{t\in(t_1,\mathrm{T}]}\left|\int_{t_1}^{\mathrm{T}}\frac{(t-u)^{\varepsilon-1}}{\Gamma(\varepsilon)}\mathbf{g}(u,\phi(u))du-\int_{t_1}^{\mathrm{T}}\frac{(t-u)^{\varepsilon-1}}{\Gamma(\varepsilon)}\mathbf{g}(u,\bar{\phi}(u))du\right| \\ &\leq \frac{\mathrm{T}^{\varepsilon}\mathbf{L_g}}{\Gamma(\varepsilon+1)}\|\phi-\bar{\phi}\|. \end{aligned} \tag{25}$$

Let $\max\left\{\mathrm{T}\mathbf{L_g},\ \frac{\mathrm{T}^{\varepsilon}\mathbf{L_g}}{\Gamma(\varepsilon+1)}\right\}=\Delta$. Then, from (24) and (25)), we have

$$\|\mathbf{N}(\phi)-\mathbf{N}(\bar{\phi})\|\leq\Delta\|\phi-\bar{\phi}\|. \tag{26}$$

As a result, an operator of contraction is $\mathbf{N}$. As a result, there is only one solution to the Problem (18).

5. Stability Theory

Here we discuss the stability results for local and global stability as well as UH stability.

5.1. Stability Results

We use the Jacobian matrix method and Lyapunov- Volterra method to prove some results for LAS and GAS of DFE and endemic equilibrium points.

Theorem 6. *The DFE point is LAS if $\mathcal{R}_0 < 1$, otherwise unstable.*

Proof. The Jacobian matrix say J at DFE $\left(\frac{\Lambda}{\eta+d}, \frac{\Lambda}{d(\eta+d)}, 0, 0, 0, 0, 0\right)$ of model (2) is given by

$$J = \begin{pmatrix} -(\eta+d) & 0 & 0 & -b(1-p\xi)\frac{\Lambda}{\eta+d} & 0 & 0 \\ \eta & -d & 0 & \frac{-wb\Lambda}{d(d+\eta)} & 0 & 0 \\ 0 & 0 & -(\tau+d) & \frac{wb\Lambda}{d(d+\eta)} + \frac{b(1-p\xi)\Lambda}{\eta+d} & 0 & 0 \\ 0 & 0 & \tau & -(\alpha_I+\sigma_I+d) & 0 & 0 \\ 0 & 0 & 0 & \sigma_I & -(\sigma_Q+\delta_Q+d) & 0 \\ 0 & 0 & 0 & \sigma_I & \sigma_Q & -d \end{pmatrix} \tag{27}$$

Computing the eigenvalues of (27), we have

$$(\lambda + (\eta+d))(\lambda+\mu)(\lambda^4 + a_1\lambda^3 + a_2\lambda^2 + a_3\lambda + a_4) = 0, \tag{28}$$

where

$a_1 = k + l + \tau + d,\ a_2 = kl + m + n + (k+l)(\tau+d),\ a_3 = km + (\tau+d)(kl+m) + nl,\ a_4 = km(\tau+d) + nm$

such that

$$\begin{aligned} k &= \sigma_I + \alpha_I + d,\ l = \sigma_Q + \delta_Q + 2d,\ m = d(\sigma_Q + \delta_Q + d), \\ n &= \frac{(\tau b(w + a(1-p\xi))\Lambda}{d(\eta+d)}. \end{aligned}$$

We see from (28) that $\lambda_1 = -(\eta+d) < 0,\ \lambda_2 = -\mu < 0$, which implies that real parts of eigenvalues are negative. It is possible to demonstrate that the eigenvalues have negative real parts by applying the Routh-Hurwitz criterion. Hence, we get from

$$\lambda^4 + a_1\lambda^3 + a_2\lambda^2 + a_3\lambda + a_4 = 0,$$

from which we see that

$$\begin{array}{lll} \lambda^4 & : & a_0 \quad a_2 \quad a_4 \\ \lambda^3 & : & b_1 \quad b_3 \quad b_5 \\ \lambda^2 & : & c_1 \quad c_3 \quad c_5 \end{array}$$

$$\begin{array}{lll} \lambda^1 & : & d_1 \quad d_3 \quad d_5 \\ \lambda^0 & : & e_1 \quad e_3 \quad e_5, \end{array}$$

where

$$\begin{aligned} b_1 &= \frac{-1}{a_1}\begin{vmatrix} a_0 & a_2 \\ a_1 & a_3 \end{vmatrix} = \frac{-(a_3 - a_1a_2)}{a_1},\ b_3 = \frac{-1}{a_1}\begin{vmatrix} a_0 & a_4 \\ a_1 & a_5 \end{vmatrix} = \frac{-(a_0a_5 - a_1a_4)}{a_1}, \\ c_1 &= \frac{-1}{b_1}\begin{vmatrix} a_1 & a_3 \\ b_1 & b_3 \end{vmatrix} = \frac{-(a_1b_3 - a_3b_1)}{b_1},\ c_3 = \frac{-1}{b_1}\begin{vmatrix} a_1 & a_5 \\ b_1 & b_5 \end{vmatrix} = \frac{-(a_1b_5 - a_5b_1)}{b_1}, \\ d_1 &= \frac{-1}{c_1}\begin{vmatrix} a_1 & a_3 \\ c_1 & c_3 \end{vmatrix} = \frac{-(a_1c_3 - a_3c_1)}{c_1},\ d_3 = \frac{-1}{c_1}\begin{vmatrix} a_1 & a_5 \\ c_1 & c_5 \end{vmatrix} = \frac{-(a_1c_5 - a_5c_1)}{c_1}, \\ e_1 &= \frac{-1}{d_1}\begin{vmatrix} a_1 & a_3 \\ d_1 & d_3 \end{vmatrix} = \frac{-(a_1d_3 - a_3d_1)}{d_1},\ e_3 = \frac{-1}{d_1}\begin{vmatrix} a_1 & a_5 \\ d_1 & d_5 \end{vmatrix} = \frac{-(a_1d_5 - a_5d_1)}{d_1}. \end{aligned}$$

By computing the above determinants, we can see that the coefficients in the first column are of same positive sign. Hence, all the roots have negative real parts. Thus the DFE is locally asymptotically stable.

Theorem 7. *The EE point $\mathcal{E}^*$ of the proposed model* (2) *is GAS in the given feasible region* Ω.

Proof. Let us define a Lyapunov function $F : \Omega \to \mathcal{R}$ by

$$\begin{aligned} F(t) &= q_1\left(S - S^* - S^*\ln\left[\frac{S}{S^*}\right]\right) \\ &+ q_2\left(V - V^* - V^*\ln\left[\frac{V}{V^*}\right]\right) \\ &+ q_3\left(E - E^* - E^*\ln\left[\frac{E}{E^*}\right]\right) \\ &= q_4\left(I - I^* - I^*\ln\left[\frac{I}{I^*}\right]\right) \\ &+ q_5\left(Q - Q^* - Q^*\ln\left[\frac{Q}{Q^*}\right]\right) \\ &+ q_6\left(R - R^* - R^*\ln\left[\frac{R}{R^*}\right]\right) \\ &+ q_7\left(D - D^* - D^*\ln\left[\frac{D}{D^*}\right]\right), \end{aligned} \tag{29}$$

where $q_i, i = 1, 2, ..., 7$ are positive constants and will be specified latter. Upon application of ${}_0^{PC}\mathrm{D}_t^{\varepsilon}$ on both sides of (29), and replacing S, V, E, I, Q, R, D by $S - S^*, V - V^*, E - E^*, I - I^*, Q - Q^*, R - R^*, D - D^8$, respectively, we have

$${}_0^{PC}\mathrm{D}_t^{\varepsilon}[F(t)] = q_1\left[\frac{S - S^*}{S}\right]{}_0^{PC}\mathrm{D}_t^{\varepsilon}S(t) + q_2\left[\frac{V - V^*}{V}\right]{}_0^{PC}\mathrm{D}_t^{\varepsilon}V(t)$$

$$
\begin{aligned}
&+ \quad q_3\left[\frac{E-E^*}{E}\right]{}_0^{PC}\mathrm{D}_t^{\varepsilon}E(t) + q_4\left[\frac{I-I^*}{I}\right]{}_0^{PC}\mathrm{D}_t^{\varepsilon}I(t)\\
&+ \quad q_5\left[\frac{Q-Q^*}{Q}\right]{}_0^{PC}\mathrm{D}_t^{\varepsilon}Q(t) + q_6\left[\frac{R-R^*}{R}\right]{}_0^{PC}\mathrm{D}_t^{\varepsilon}R(t)\\
&+ \quad q_7\left[\frac{D-D^*}{D}\right]{}_0^{PC}\mathrm{D}_t^{\varepsilon}D(t). \qquad (30)
\end{aligned}
$$

By choosing $q_i = 1$, for $i = 1, 2, ..., 7$, and plugging values from (2) in (30), and separating positive and negative parts, such that

$$
\begin{aligned}
\Theta_1 &= \Lambda\frac{S-S^*}{S} + \eta\frac{(V-V^*)(S-S^*)}{V} + wb\frac{(E-E^*)(V-V^*)(I-I^*)}{E}\\
&+ b(1-p\xi)\frac{(S-S^*)(I-I^*)(E-E^*)}{E} + \tau\frac{(E-E^*)(I-I^*)}{I} + \alpha_I\frac{(Q-Q^*)(I-I^*)}{Q} \qquad (31)\\
&+ \sigma_I(R-R^*)\frac{(I-I^*)}{R} + \sigma_Q\frac{(Q-Q^*)(R-R^*)}{R} + \delta_I\frac{(D-D^*)(I-I^*)}{D}\\
&+ \delta_Q\frac{(Q-Q^*)(D-D^*)}{D},
\end{aligned}
$$

and

$$
\begin{aligned}
\Theta_2 &= b(1-p\xi)\frac{(S-S^*)^2(I-I^*)}{S} + (\eta+d)\frac{(S-S^*)^2}{S} + wb\frac{(E-E^*)(V-V^*)^2(I-I^*)}{V}\\
&+ \frac{d(V-v^*)^2}{V} + (\tau+d)\frac{(E-E^*)^2}{E} + (\alpha_I+\delta_I+\sigma_I+d)\frac{(I-I^*)^2}{I} \qquad (32)\\
&+ (\sigma_Q+\delta_Q+d)\frac{(Q-Q^*)^2}{Q} + d\frac{(R-R^*)^2}{R}.
\end{aligned}
$$

Using (31), and (32) in (30), we have

$$
{}_0^{PC}\mathrm{D}_t^{\varepsilon}[F(t)] = \Theta_1 - \Theta_2. \qquad (33)
$$

We see that in (33) if $\Theta_1 < \Theta_2$, then ${}_0^{PC}\mathrm{D}_t^{\varepsilon}[F(t)] \leq 0$, Hence the Lyapunov- Volterra function F is negative under the derivative of piecewise. But $F > 0$, therefore F is positive definite function, therefore, the endemic equilibrium point $\mathcal{E}^*$ is GAS.

5.2. UH Stability

The UH stability results are derived in this portion.

Remark 1. *If* $\mathbf{h}$ *is a function that is independent of* ϕ*, then* $\mathbf{h} : \mathcal{J} \to (0, \infty),\ \ni \mathbf{h}(0) = \mathbf{h}(t_1) = 0$ *and*

$$
|\mathbf{h}(t)| \leq \epsilon, \quad \textit{for every } t \in \mathcal{J}.
$$

Lemma 4. *The*

$$\begin{aligned} {}_0^{PC}\mathrm{D}_t^{\varepsilon}\phi(t) &= \mathbf{g}(t,\phi(t))+\mathbf{h}(t), \quad 0<\varepsilon\leq 1,\\ \phi(0) &= \phi_0 \end{aligned}$$

yield a result of the form

$$\phi(t)=\begin{cases}\phi_0+\displaystyle\int_0^t \mathbf{g}(u,\phi(u))du+\int_0^t \mathbf{h}(u)du,\ t\in\nabla_1,\\ \phi(t_1)+\displaystyle\int_{t_1}^{\mathrm{T}}\frac{(t-u)^{\varepsilon-1}}{\Gamma(\varepsilon)}\mathbf{g}(u,\phi(u))d(u)+\int_{t_1}^{\mathrm{T}}\frac{(t-u)^{\varepsilon-1}}{\Gamma(\varepsilon)}\mathbf{h}(u)du, \quad t\in\nabla_2.\end{cases} \tag{34}$$

Moreover, the solution (34) *satisfies the following relation in view of Remark 1 and using* $|\mathrm{T}-t_1|\leq \mathrm{T}$ *as*

$$\begin{aligned} \left|\phi(t)-\phi_0-\int_0^t \mathbf{g}(u,\phi(u))du\right| &\leq t_1\epsilon,\ t\in\nabla_1,\\ \left|\phi(t)-\phi(t_1)-\int_{t_1}^{\mathrm{T}}\frac{(t-u)^{\varepsilon-1}}{\Gamma(\varepsilon)}\mathbf{g}(u,\phi(u))du\right| &\leq \frac{\mathrm{T}^{\varepsilon}\epsilon}{\Gamma(\varepsilon+1)},\ t\in\nabla_2. \end{aligned}$$

Proof. The proof of the Lemma 4 is easy to derive.

Theorem 8. *We get UH and generalized UH stable if the condition* $\max\left\{1-t_1\mathbf{L_g}, 1-\bar{\Delta}\right\}<1$, *where* $\bar{\Delta}=\frac{\mathrm{T}^{\varepsilon}\mathbf{L_g}}{\Gamma(\varepsilon+1)}$ *holds corresponding to the solution of problem* (18).

Proof. We derive proof in two steps:
Step I: $t\in[0,t_1]$, then

$$\begin{aligned} \left\|\phi-\bar{\phi}\right\| &= \max_{t\in\mathcal{J}}\left|\phi(t)-\phi_0-\int_0^t \mathbf{g}(u,\bar{\phi}(u))du\right|\\ &\leq \max_{t\in\mathcal{J}}\left|\phi(t)-\phi_0-\int_0^t \mathbf{g}(u,\phi(u))du\right|\\ &+ \max_{t\in\mathcal{J}}\left|\int_0^t \mathbf{g}(u,\phi(u))du-\int_0^t \mathbf{g}(u,\bar{\phi}(u))du\right|\\ &\leq \epsilon t_1+\mathbf{L_g}t_1\|\phi-\bar{\phi}\|. \end{aligned} \tag{35}$$

Hence from (35), we get

$$\left\|\phi-\bar{\phi}\right\| \leq \frac{\epsilon t_1}{1-t_1\mathbf{L_g}}. \tag{36}$$

Step II: If $t \in [\mathrm{t}_1, \mathrm{T}]$, then we have

$$\begin{aligned}
\left\|\phi - \bar{\phi}\right\| &= \max_{t\in\mathcal{J}} \left|\phi(t) - \phi(t_1) - \int_{t_1}^{\mathrm{T}} \frac{(t-u)^{\varepsilon-1}}{\Gamma(\varepsilon)}\mathbf{g}(u, \bar{\phi}(u))du\right| \\
&\leq \max_{t\in\mathcal{J}} \left|\phi(t) - \phi(t_1) - \int_{t_1}^{\mathrm{T}} \frac{(t-u)^{\varepsilon-1}}{\Gamma(\varepsilon)}\mathbf{g}(u, \phi(u))du\right| \\
&+ \max_{t\in\mathcal{J}} \left|\int_{t_1}^{\mathrm{T}} \frac{(t-u)^{\varepsilon-1}}{\Gamma(\varepsilon)}\mathbf{g}(u, \phi(u))du - \int_{t_1}^{\mathrm{T}} \frac{(t-u)^{\varepsilon-1}}{\Gamma(\varepsilon)}\mathbf{g}(u, \bar{\phi}(u))du\right| \\
&\leq \frac{\mathrm{T}^{\varepsilon}\epsilon}{\Gamma(\varepsilon+1)} + \frac{\mathrm{T}^{\varepsilon}\mathbf{L_g}}{\Gamma(\varepsilon+1)}\|\phi - \bar{\phi}\|. \qquad (37)
\end{aligned}$$

From (37),

$$\left\|\phi - \bar{\phi}\right\| \leq \left[\frac{\mathrm{T}^{\varepsilon}}{(1-\bar{\Delta})\Gamma(\varepsilon+1)}\right]\epsilon. \qquad (38)$$

We can now see that the solution to issue (18) is UH stable based on (36) and (38). Moreover, the solution is unquestionably generalized UH stable if there is a non-decreasing function $\Phi : \mathcal{J} \to [0, \infty)$ such that $\Phi(\epsilon) = \epsilon$.

6. Numerical Scheme

Here, we expand the approach from [24] to build the numerical scheme based on the RKm method of order four. For computation purposes, where small steps are to be computed the Euler method is good. However, for evaluations of largen numbers of steps, the RKm method is given preferred because in such a situation it gives efficient and accurate solution. In light of this need, we view the fractional order problem as

$$\begin{aligned}
{}_0^{PC}D_t^{\varepsilon}\phi(t) &= \mathbf{g}_j(t, \phi(t)),\ j = 1, 2, ..., 7 \\
\phi(0) &= \phi_0. \qquad (39)
\end{aligned}$$

where $\mathbf{g}_j : \mathcal{J} \times \mathbb{R} \to \mathbb{R}$. We may express Taylor series in general form as

$$\phi(t+h) = \phi(t) + \frac{h^{\varepsilon}}{\Gamma(\varepsilon+1)}\mathrm{D}_t{}^{\varepsilon}\phi(t) + \frac{h^{2\varepsilon}}{\Gamma(2\varepsilon+1)}\mathrm{D}_t^{2\varepsilon}x(t) + ... \qquad (40)$$

On applying $\mathrm{D}_t{}^{2\varepsilon}\phi = \mathrm{D}_t\mathbf{g}_j(t, \phi(t)) + \mathbf{g}_j(t, \phi(t))\mathrm{D}_{\phi}{}^{\varepsilon}\mathbf{g}(t, \phi(t))$ in (40) implies the following results:

$$\phi_{i+1} = \phi_i + \frac{h^{\varepsilon}}{\Gamma(\varepsilon+1)}\mathbf{g}_j(t_i, \phi(t_i)) + \frac{h^{\varepsilon}}{2\Gamma(\varepsilon+1)}\left[\mathcal{K}_1 + \mathcal{K}_2\right], \qquad (41)$$

where

$$\mathcal{K}_1 = \mathbf{g}_j(t_i, \phi_i(t_i)),\ \mathcal{K}_2 = \mathbf{g}_j\left(t_i + \frac{2h^{\varepsilon}\Gamma(\varepsilon+1)}{\Gamma(2\varepsilon+1)},\ \phi(t_i) + \frac{2h^{\varepsilon}\Gamma(\varepsilon+1)}{\Gamma(2\varepsilon+1)}\mathbf{g}_j(t_i, \phi_i(t_i))\right). \qquad (42)$$

On using $\varepsilon = 1$, gives ordinary numerical method.

To illustrate the compartmental solutions graphically, we derive numerical scheme as:

$$\mathbf{S}(t_{i+1})) = \begin{cases} \mathbf{S}_{i-1}(t_{i-1}) + \dfrac{h}{2}\mathbf{g}_1\left[t_{i-1} + \dfrac{h}{2},\ \phi_{i-1}(t_{i-1}) + \dfrac{\mathcal{K}_1}{2}\right], & t \in \nabla_1 \\ \mathbf{S}_i(t_i) + \dfrac{h^{\varphi}}{\Gamma(\varepsilon+1)}\mathbf{g}_1(t_i,\ \phi_i(t_i)) + \dfrac{h^{\varepsilon}}{2\Gamma(\varepsilon+1)}\left[\mathcal{K}_2 + \mathcal{K}_3\right], & t \in \nabla_2, \end{cases} \tag{43}$$

where $h = t_{i+1} - t_i$ and

$$\begin{aligned} \mathcal{K}_1 &= \mathbf{g}_1(t_{i-1},\ \phi_{i-1}(t_{i-1})), \quad \mathcal{K}_2 = \mathbf{g}_1(t_i,\ \phi_i(t_i)), \\ \mathcal{K}_3 &= \mathbf{g}_1\left(t_i + \frac{2h^{\varepsilon}\Gamma(\varepsilon+1)}{\Gamma(2\varepsilon+1)},\ \phi(t_i) + \frac{2h^{\varepsilon}\Gamma(\varepsilon+1)}{\Gamma(2\varepsilon+1)}\mathbf{g}_1(t_i,\ \phi_i(t_i))\right). \end{aligned} \tag{44}$$

With the same patron

$$\mathbf{V}(t_{i+1})) = \begin{cases} \mathbf{V}_{i-1}(t_{i-1}) + \dfrac{h}{2}\mathbf{g}_2\left[t_{i-1} + \dfrac{h}{2},\ \phi_{i-1}(t_{i-1}) + \dfrac{\mathcal{K}_1}{2}\right], & t \in \nabla_1 \\ \mathbf{V}_i(t_i) + \dfrac{h^{\varepsilon}}{\Gamma(\varepsilon+1)}\mathbf{g}_2(t_i,\ \phi_i(t_i)) + \dfrac{h^{\varepsilon}}{2\Gamma(\varepsilon+1)}\left[\mathcal{K}_2 + \mathcal{K}_3\right], & t \in \nabla_2, \end{cases} \tag{45}$$

$$\mathbf{E}(t_{i+1})) = \begin{cases} \mathbf{E}_{i-1}(t_{i-1}) + \dfrac{h}{2}\mathbf{g}_3\left[t_{i-1} + \dfrac{h}{2},\ \phi_{i-1}(t_{i-1}) + \dfrac{\mathcal{K}_1}{2}\right], & t \in \nabla_1 \\ \mathbf{E}_i(t_i) + \dfrac{h^{\varepsilon}}{\Gamma(\varepsilon+1)}\mathbf{g}_3(t_i,\ \phi_i(t_i)) + \dfrac{h^{\varepsilon}}{2\Gamma(\varepsilon+1)}\left[\mathcal{K}_2 + \mathcal{K}_3\right], & t \in \nabla_2, \end{cases} \tag{46}$$

$$\mathbf{I}(t_{i+1})) = \begin{cases} \mathbf{I}_{i-1}(t_{i-1}) + \dfrac{h}{2}\mathbf{g}_4\left[t_{i-1} + \dfrac{h}{2},\ \phi_{i-1}(t_{i-1}) + \dfrac{\mathcal{K}_1}{2}\right], & t \in \nabla_1 \\ \mathbf{I}_i(t_i) + \dfrac{h^{\varepsilon}}{\Gamma(\varepsilon+1)}\mathbf{g}_4(t_i,\ \phi_i(t_i)) + \dfrac{h^{\varepsilon}}{2\Gamma(\varepsilon+1)}\left[\mathcal{K}_2 + \mathcal{K}_3\right], & t \in \nabla_2, \end{cases} \tag{47}$$

$$\mathbf{Q}(t_{i+1})) = \begin{cases} \mathbf{Q}_{i-1}(t_{i-1}) + \dfrac{h}{2}\mathbf{g}_5\left[t_{i-1} + \dfrac{h}{2},\ \phi_{i-1}(t_{i-1}) + \dfrac{\mathcal{K}_1}{2}\right], & t \in \nabla_1 \\ \mathbf{R}_i(t_i) + \dfrac{h^{\varepsilon}}{\Gamma(\varepsilon+1)}\mathbf{g}_5(t_i,\ \phi_i(t_i)) + \dfrac{h^{\varepsilon}}{2\Gamma(\varepsilon+1)}\left[\mathcal{K}_2 + \mathcal{K}_3\right], & t \in \nabla_2, \end{cases} \tag{48}$$

$$\mathbf{R}(t_{i+1})) = \begin{cases} \mathbf{R}_{i-1}(t_{i-1}) + \dfrac{h}{2}\mathbf{g}_6\left[t_{i-1} + \dfrac{h}{2},\ \phi_{i-1}(t_{i-1}) + \dfrac{\mathcal{K}_1}{2}\right], & t \in \nabla_1 \\ \mathbf{R}_i(t_i) + \dfrac{h^{\varepsilon}}{\Gamma(\varepsilon+1)}\mathbf{g}_6(t_i,\ \phi_i(t_i)) + \dfrac{h^{\varepsilon}}{2\Gamma(\varepsilon+1)}\left[\mathcal{K}_2 + \mathcal{K}_3\right], & t \in \nabla_2, \end{cases} \tag{49}$$

and

$$\mathbf{D}(t_{i+1})) = \begin{cases} \mathbf{D}_{i-1}(t_{i-1}) + \dfrac{h}{2}\mathbf{g}_7\left[t_{i-1} + \dfrac{h}{2},\ \phi_{i-1}(t_{i-1}) + \dfrac{\mathcal{K}_1}{2}\right], & t \in \nabla_1 \\ \mathbf{D}_i(t_i) + \dfrac{h^{\varepsilon}}{\Gamma(\varepsilon+1)}\mathbf{g}_7(t_i,\ \phi_i(t_i)) + \dfrac{h^{\varepsilon}}{2\Gamma(\varepsilon+1)}\left[\mathcal{K}_2 + \mathcal{K}_3\right], & t \in \nabla_2. \end{cases} \tag{50}$$

7. Graphical Illustrations and Explanations

To simulate our results graphically, we use the numerical values of table 1 and taking the initial data as given by $S(0) = 97.00000;\ V(0) = 50.00000;\ E(0) = 70.00000;\ I(0) = 1.581936;\ Q(0) = 1.581936;\ R(0) = 1.538689;\ D(0) = 0.030664.$

7.1. Case-I

We take the first set of fractional order values in $(0.60, 0.80]$ and presented solutions graphically in figures 4, 5, 6, 7, 8, 9, 10 respectively.

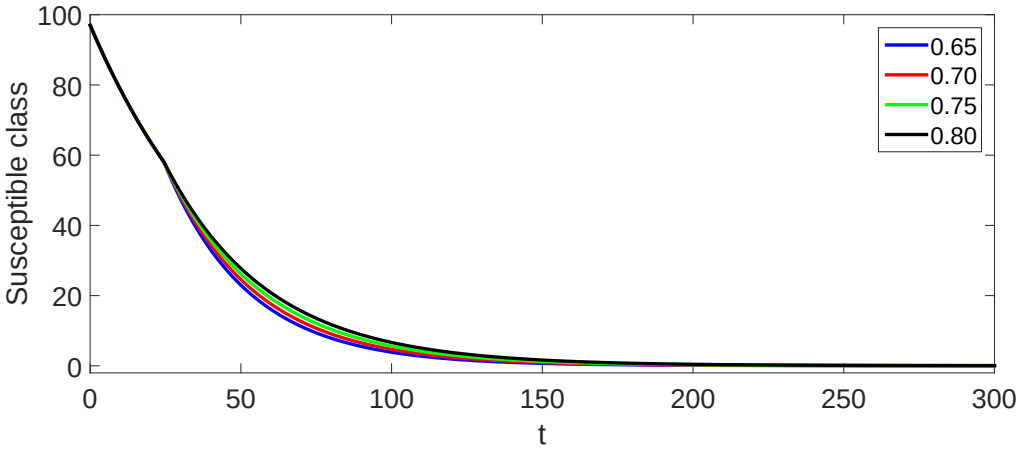

Figure 4: Solution illustration of susceptible class for $\varepsilon \in (0.60, 0.80]$.

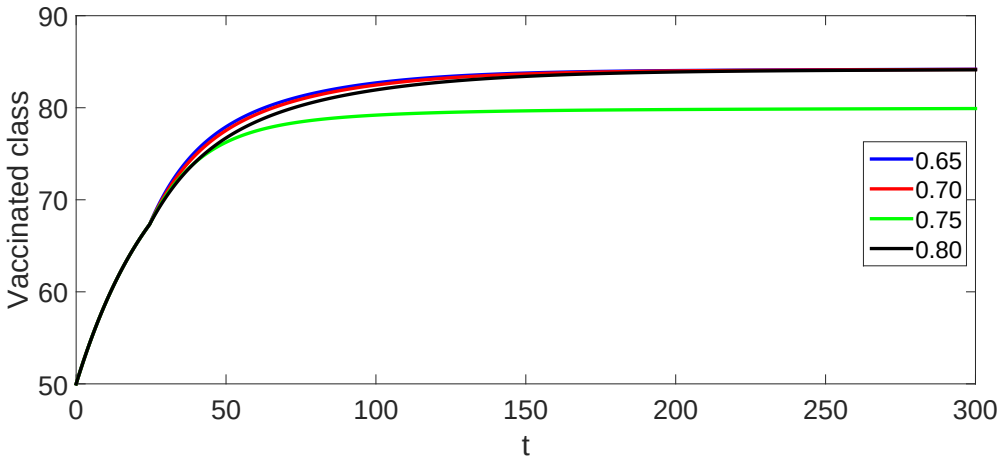

Figure 5: Solution illustration of vaccinated class for $\varepsilon \in (0.60, 0.80]$.

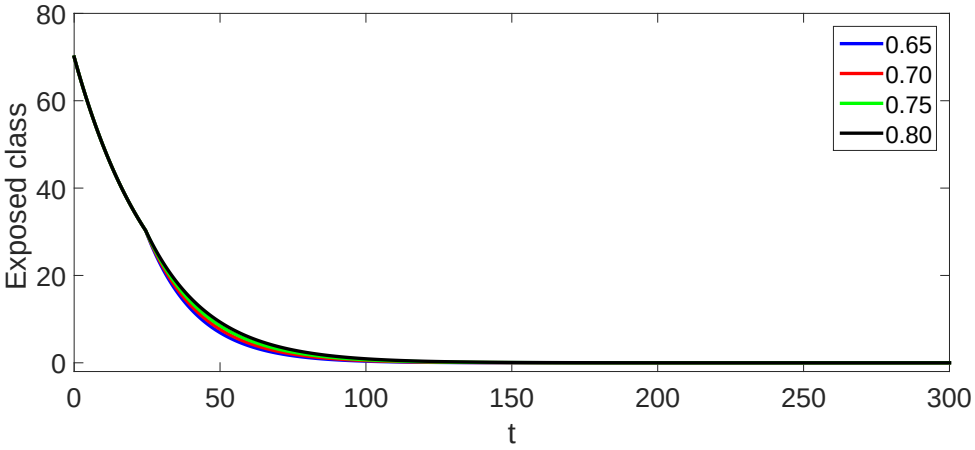

Figure 6: Solution illustration of exposed class for $\varepsilon \in (0.60, 0.80]$.

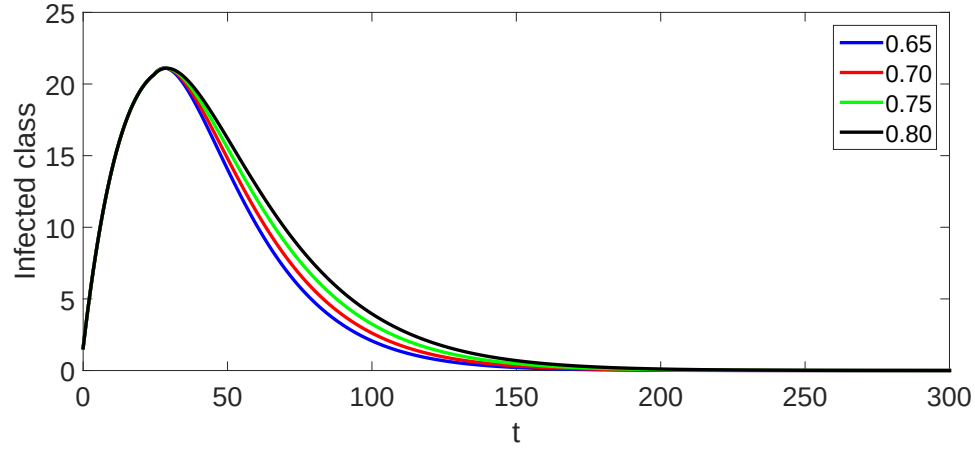

Figure 7: Solution illustration of infected class for $\varepsilon \in (0.60, 0.80]$.

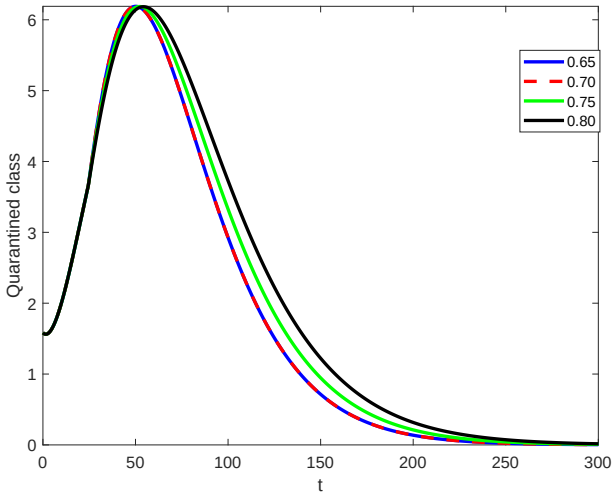

Figure 8: Solution illustration of quarantined class for $\varepsilon \in (0.60, 0.80]$.

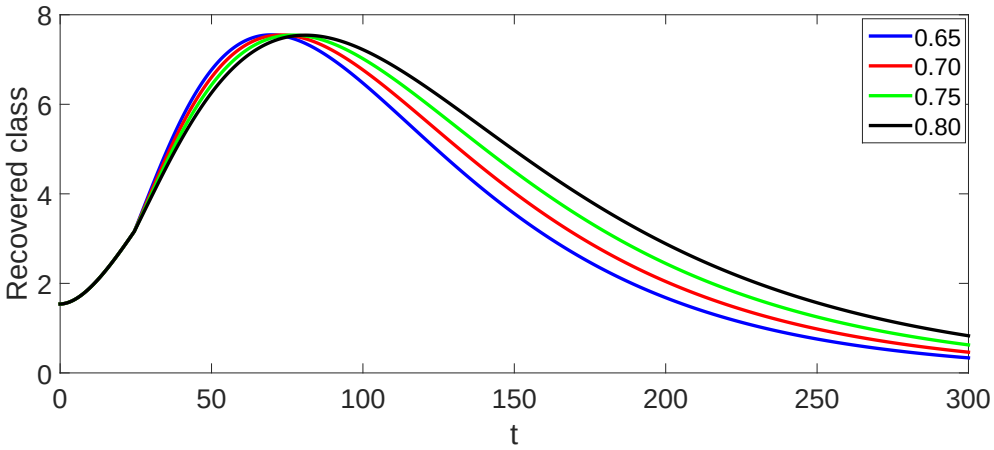

Figure 9: Solution illustration of recovered class for $\varepsilon \in (0.60, 0.80]$.

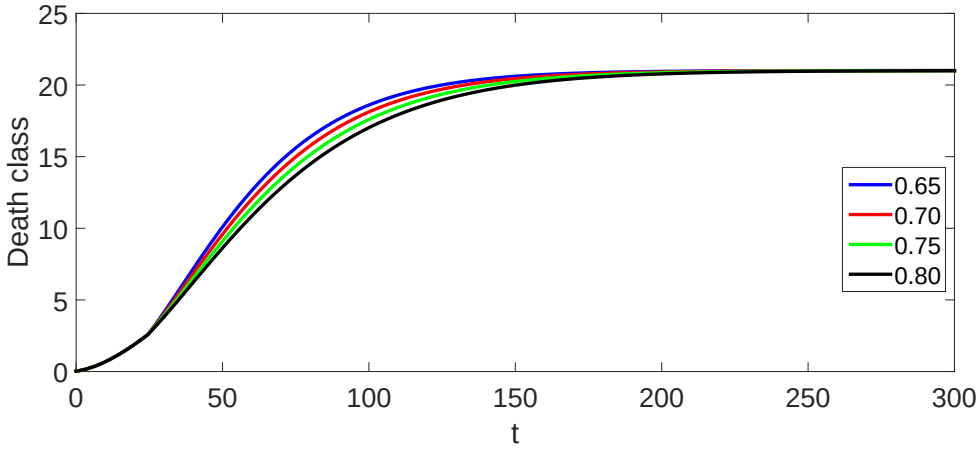

Figure 10: Solution illustration of death class for $\varepsilon \in (0.60, 0.80]$.

In the above graphical presentations, we have taken $t_1 < 50$, and T = 300, the corresponding crossover effect can be observed near the point $t_1 < 50$ in all compartments. The susceptible population is decreasing, in the same vaccinated classes has raised. On the other hand exposed class was reducing as infection was spreading in the society. In the mean time quarantined initially risen and then went on on decreasing. The recovered individuals were increasing with the passage of time and also the death class has grown. In all compartment stability after some time occurred.

7.2. Case-II

We take the first set of fractional order values in $(0.80, 1.00]$ and presented solutions graphically in figures 11, 12, 13, 14, 15, 16, 17 respectively.

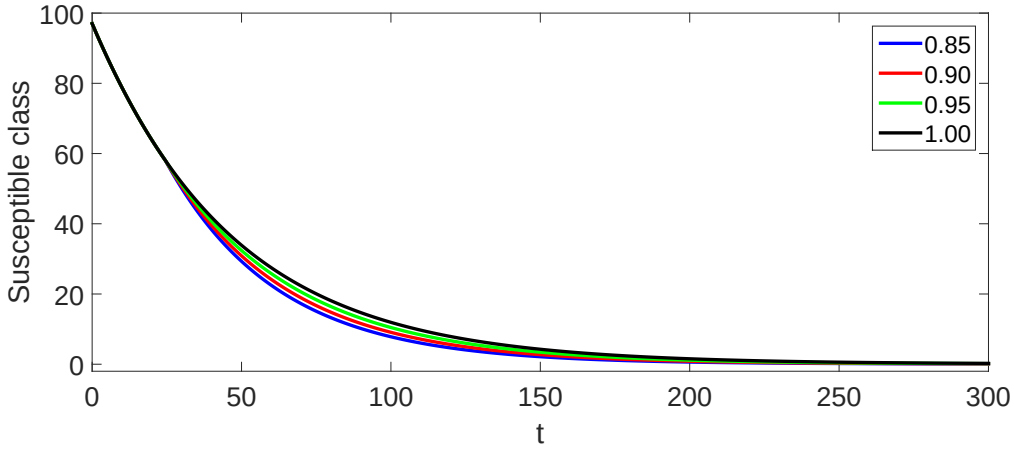

Figure 11: Solution illustration of susceptible class for $\varepsilon \in (0.80, 1.00]$.

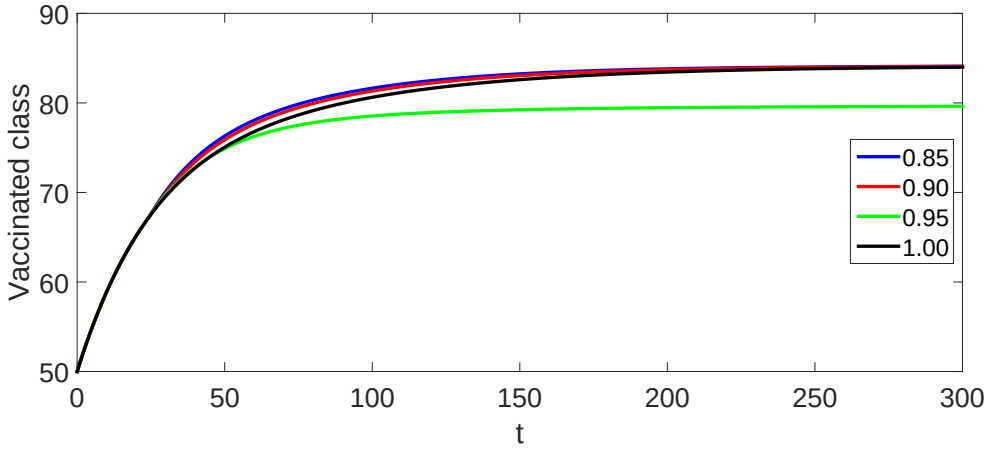

Figure 12: Solution illustration of vaccinated class for $\varepsilon \in (0.80, 1.00]$.

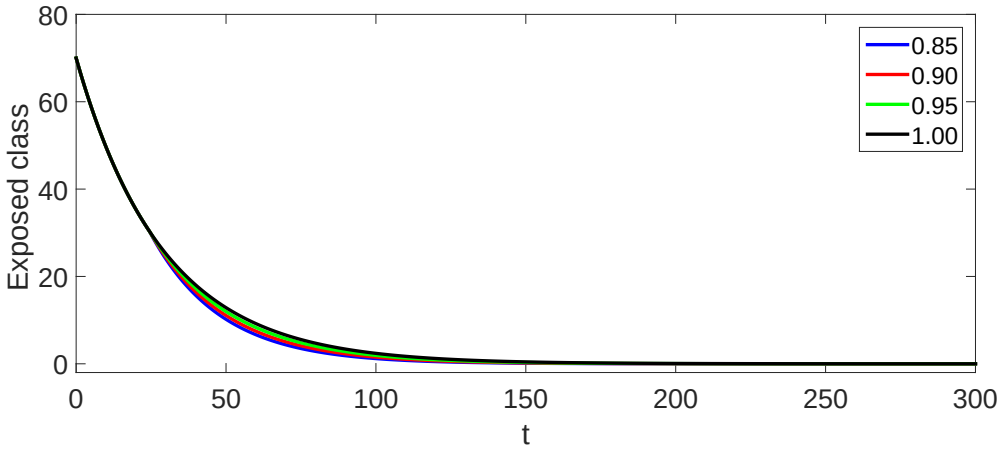

Figure 13: Solution illustration of exposed class for $\varepsilon \in (0.80, 1.00]$.

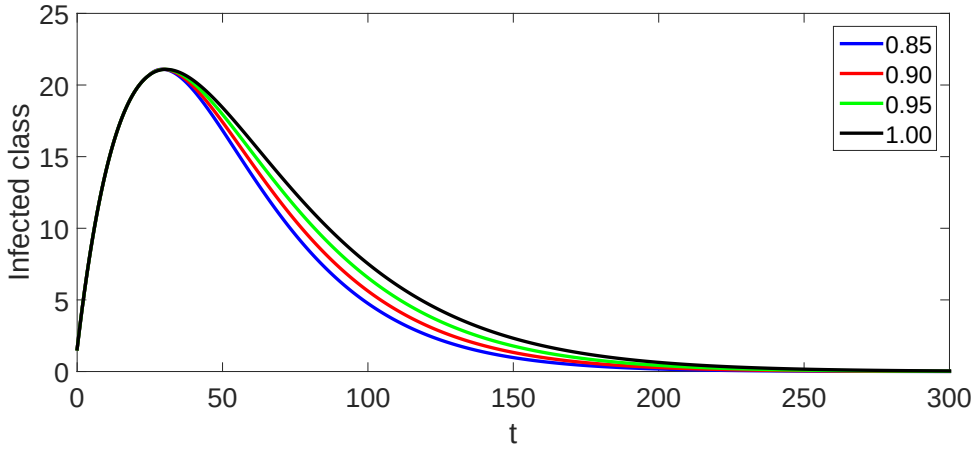

Figure 14: Solution illustration of infected class for $\varepsilon \in (0.80, 1.00]$.

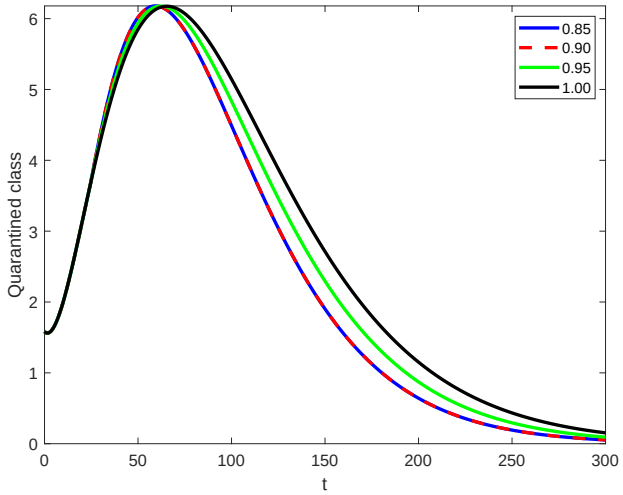

Figure 15: Solution illustration of quarantined class for $\varepsilon \in (0.80, 1.00]$.

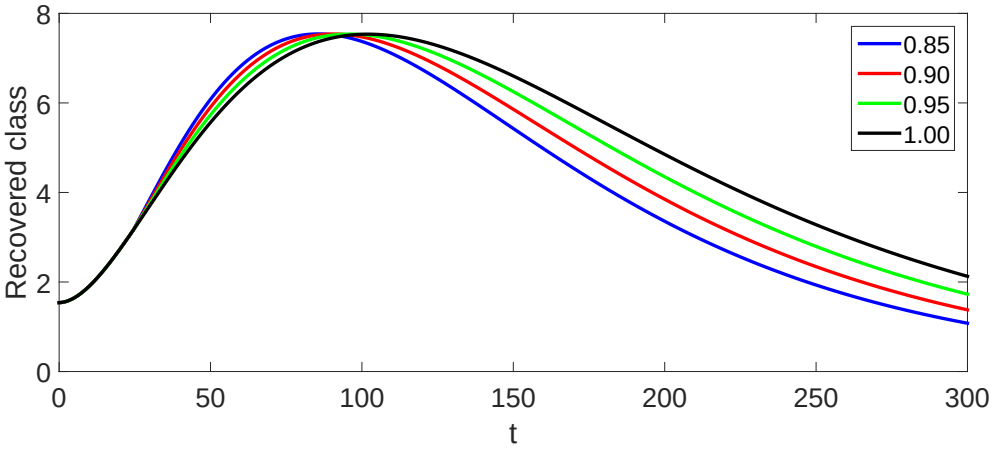

Figure 16: Solution illustration of recovered class for $\varepsilon \in (0.80, 1.00]$.

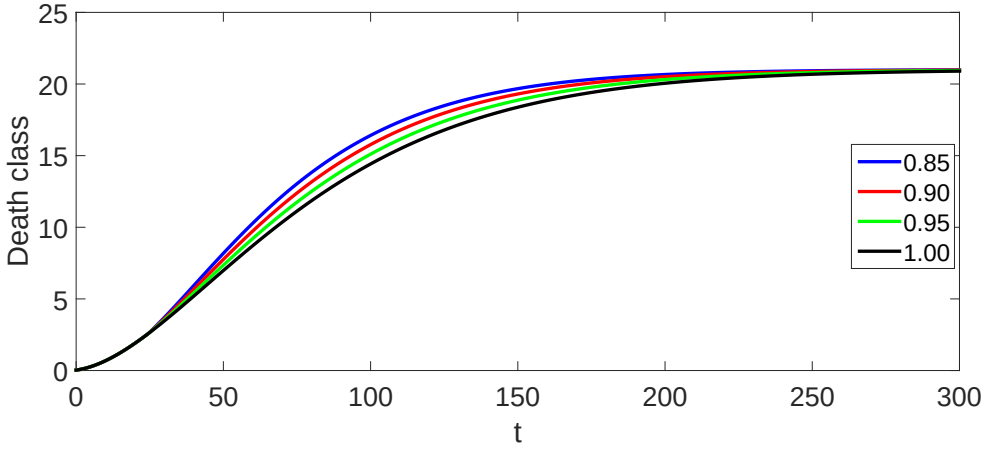

Figure 17: Solution illustration of death class for $\varepsilon \in (0.80, 1.00]$.

Given $t_1 < 50$ and T = 300 in the graphical displays above, the relevant crossover effect is visible in all compartments close to $t_1 < 50$. In the same classes that have increased in vaccinations, the vulnerable population is declining. On the other hand, as infection increased throughout society, the exposed class shrank. Quarantined cases increased in the interim before continuing to decline. Over time, both the number of recovered individuals and the number of deaths have increased. After a while, stability happened in every compartment. From the figures given above, we see that the decay dynamics is faster at lower values of fractional orders while in case of growth, the dynamic is rapidly increasing under the larger values of fractional orders. In the same way, the growth in dynamics is slower at small fractional orders and faster at higher values. This chastities demonstrate the influence of fractional orders on the dynamical behaviours of various classes.

8. Conclusion

With the help of new recently introduced concepts of fractional calculus, we have investigated a determinacy mathematical model of COVID-19. Because such modeling is very effective if the involve parameters and functions are suitably defined. Additionally, if the parameters can be accurately approximated, epidemic modeling is a very useful method for estimating the state of the COVID-19 worldwide pandemic. Keeping these things in mind, we have revisited a mathematical model [29] under the piecewise fractional order derivative. Fundamental results including positivity, boundedness and equilibrium points were deduced. Also reproductive numbers was calculated. Here, we have investigated sensitivity analysis of the model via reproductive number analysis. We observe that increase the value value of percentage upto some extent can increase or decrease the sensitivity index by that percent. The existence theory is an important tool to be investigated for dynamical problem. Here, we have used Schauder's and Banach fixed point theorems to establish a detailed analysis for existence theory of solution to the proposed model. Additional stability is important consequence and for dynamical systems two kinds of stability be studied. One is devoted to stability of equilibrium points which is global or local in nature. Therefore, we have attempted to deduce some results related to local asymptotically stability of DFE point. It was deduced that DFE point is asymptotically stable if $\mathcal{R}_0 < 1$. On the other hand Laypunov-Volterra theory was used to show some results for global stability of endemic equilibrium point. The second stability results were devoted to numerical type. Hence, we have used UH concepts to deduce such results. Finally, a sophisticated numerical algorithm was derived by using the RK2 method. We have used this scheme to simulate our results graphically. We see that crossover behaviors can seen in each compartment after t_1 in their graphical presentation.

In the future, we can investigate the mentioned models from different perspectives like:

- By using fractals fractional calculus the considered model has not studied.
- On applying the traditional tools of fractional calculus in terms of conformable can be investigated.
- We can investigate the model by using non-singular type derivatives.
- Stochastic form of this model has not yet studied.
- In the future, if we include the harmonic mean type nonlinear incidence rate to properly investigate the disease dynamics.

In the future, we will extend the numerical schemes introduced in [2–4] for piecewise derivatives of fractional orders using different kinds of definitions.

Acknowledgements

We are thankful to Prince Sultan University for support through TAS research lab.

References

[1] R. P. Agarwal. *Fixed Point Theory and Applications*. Cambridge University Press, 2001.

[2] N. Almutairi and S. Saber. Chaos control and numerical solution of time-varying fractional newton-leipnik system using fractional atangana-baleanu derivatives. *AIMS Mathematics*, 8(11):25863–25887, 2023.

[3] N. Almutairi and S. Saber. On chaos control of nonlinear fractional newton-leipnik system via fractional caputo-fabrizio derivatives. *Scientific Reports*, 13(1):22726, 2023.

[4] N. Almutairi and S. Saber. Application of a time-fractal fractional derivative with a power-law kernel to the burke-shaw system based on newton's interpolation polynomials. *MethodsX*, 12:102510, 2024.

[5] M. H. Aqlan, A. Alsaedi, B. Ahmad, and J. J. Nieto. Mathematical modeling and prediction in infectious disease epidemiology. *Open Mathematics*, 14(1):723–735, 2016.

[6] A. Atangana. Modelling the spread of covid-19 with new fractal-fractional operators: Can the lockdown save mankind before vaccination? *Chaos, Solitons Fractals*, 136:109860, 2020.

[7] A. Atangana and S. I. Araz. New concept in calculus: Piecewise differential and integral operators. *Chaos, Solitons Fractals*, 145:110638, 2021.

[8] A. Atangana and S. I. Araz. Rhythmic behaviors of the human heart with piecewise derivative. *Mathematical Biosciences and Engineering*, 19:3091–3109, 2022.

[9] A. Atangana and S. I. Araz. Piecewise differential equations: Theory, methods and applications. *AIMS Mathematics*, 8(7):15352–15382, 2023.

[10] N. Bacaer. *A Short History of Mathematical Population Dynamics*. Springer, London, 2011.

[11] F. Brauer, C. Castillo-Chavez, and Z. Feng. *Mathematical Models in Epidemiology*. Springer, New York, 2019.

[12] C. Chen, M. Bohner, and B. Jia. Ulam-hyers stability of caputo fractional difference equations. *Mathematical Methods in the Applied Sciences*, 42(18):7461–7470, 2019.

[13] A. K. Cheng. *Mathematical modelling and real life problem solving*. Association of Mathematics Educators, 2009.

[14] Y. J. Cho. Survey on metric fixed point theory and applications. *Advances in Real and Complex Analysis with Applications*, pages 183–241, 2017.

[15] M. Dalir and M. Bashour. Applications of fractional calculus. *Applied Mathematical Sciences*, 4(21):1021–1032, 2011.

[16] L. Edelstein-Keshet. *Mathematical Models in Biology*. SIAM, 2004.

[17] A. Granas and J. Dugundji. *Fixed Point Theory*, volume 14. Springer, New York, 2003.

[18] A. B. Gumel, S. Ruan, T. Day, J. Watmough, F. Brauer, P. van den Driessche, D. Gabrielson, C. Bowman, M. E. Alexander, S. Ardal, and J. Wu. Modelling strategies for controlling sars outbreaks. *Proceedings of the Royal Society of London. Series B: Biological Sciences*, 1554:2223–2232, 2004.

[19] A. Huppert and G. Katriel. Mathematical modeling and prediction in infectious disease epidemiology. *Clinical Microbiology and Infection*, 19(11):999–1005, 2013.
[20] R. M. Jena. *Piecewise concept in fractional models*. Academic Press, New York, 2024.
[21] H. Khan, S. Ahmad, J. Alzabut, and A. T. Azar. A generalized coupled system of fractional differential equations with application to finite time sliding mode control for leukemia therapy. *Chaos, Solitons Fractals*, 174:113901, 2023.
[22] H. Khan, J. Alzabut, W. F. Alfwzan, and H. Gulzar. Nonlinear dynamics of a piecewise modified abc fractional-order leukemia model with symmetric numerical simulations. *Symmetry*, 15(7):1338, 2023.
[23] H. Khan, J. Alzabut, J. F. Gomez-Aguilar, and R. P. Agarwal. Piecewise mabc fractional derivative with an application. *AIMS Mathematics*, 8(10):24345–24366, 2023.
[24] S. Khan, Z. A. Khan, H. Alrabaiah, and S. Zeb. On using piecewise fractional differential operator to study a dynamical system. *Axioms*, 12(3):292, 2023.
[25] S. Khan, K. Shah, A. Debbouche, S. Zeb, and V. Antonov. Solvability and ulam-hyers stability analysis for nonlinear piecewise fractional cancer dynamic systems. *Physica Scripta*, 99(2):025225, 2024.
[26] V. Kiryakova. The special functions of fractional calculus as generalized fractional calculus operators of some basic functions. *Computers Mathematics with Applications*, 59(3):1128–1141, 2020.
[27] R. L. Magin. Fractional calculus in bioengineering: A tool to model complex dynamics. In *Proceedings of the 13th International Carpathian Control Conference (ICCC)*, pages 464–469. IEEE, 2012.
[28] M. Meerschaert. *Mathematical Modeling*. Academic Press, New York, 2013.
[29] C. Photphanloet, S. Ritraksa, S. E. Shuaib, A. Intarasit, and P. Riyapan. A compartmental model for assessing effects of covid-19 vaccination in thailand. *Universal Journal of Public Health*, 10(6):596–605, 2022.
[30] S. S. Redhwan, M. Han, M. A. Almalahi, M. A. Alyami, M. Alsulami, and N. Alghamdi. Piecewise implicit coupled system under abc fractional differential equations with variable order. *AIMS Mathematics*, 9(6):15303–15324, 2024.
[31] M. Roccetti. Drawing a parallel between the trend of confirmed covid-19 deaths in the winters of 2022/2023 and 2023/2024 in italy, with a prediction. *Mathematical Biosciences and Engineering*, 21(3):3742–3754, 2024.
[32] B. Ross. A brief history and exposition of the fundamental theory of fractional calculus. In *Fractional Calculus and Its Applications*. Springer, Berlin, 1975.
[33] I. A. Rus. *Ulam stability of the operatorial equations*. Springer, New York, 2011.
[34] M. A. Sanchez and S. M. Blower. Uncertainty and sensitivity analysis of the basic reproductive rate: Tuberculosis as an example. *American Journal of Epidemiology*, 145(12):1127–1137, 1997.
[35] F. Schaffner and A. Mathis. Dengue and dengue vectors in the who european region: past, present, and scenarios for the future. *The Lancet Infectious Diseases*, 14(12):1271–1280, 2014.
[36] K. Shah, T. Abdeljawad, and A. Ali. Mathematical analysis of the cauchy type

dynamical system under piecewise equations with caputo fractional derivative. *Chaos, Solitons Fractals*, 161:112356, 2022.

[37] K. Shah, A. Khan, B. Abdalla, T. Abdeljawad, and K. A. Khan. A mathematical model for nipah virus disease by using piecewise fractional order caputo derivative. *Fractals*, 32(02):2440013, 2024.

[38] K. Shah, A. Khan, B. Abdalla, T. Abdeljawad, and K. A. Khan. A mathematical model for nipah virus disease by using piecewise fractional order caputo derivative. *Fractals*, 32(2):2440013, 2024.

[39] K. Shah, P. Kumam, and I. Ullah. On ulam stability and multiplicity results to a nonlinear coupled system with integral boundary conditions. *Mathematics*, 7(3):223, 2019.

[40] K. Shah, H. Naz, T. Abdeljawad, and B. Abdalla. Study of fractional order dynamical system of viral infection disease under piecewise derivative. *CMES-Computer Modeling in Engineering Sciences*, 136(1):921–941, 2023.

[41] N. H. Tuan, H. Mohammadi, and S. Rezapour. A mathematical model for covid-19 transmission by using the caputo fractional derivative. *Chaos, Solitons Fractals*, 140:110107, 2020.

[42] V. V. Uchaikin. *Fractional Derivatives for Physicists and Engineers*, volume 2. Springer, Berlin, 2013.

[43] C. Vargas-De-León. Volterra-type lyapunov functions for fractional-order epidemic systems. *Communications in Nonlinear Science and Numerical Simulation*, 24(1-3):75–85, 2015.

[44] J. T. Wu, K. Leung, and G. M. Leung. Nowcasting and forecasting the potential domestic and international spread of the 2019-ncov outbreak originating in wuhan, china: a modelling study. *The Lancet*, 395(10225):689–697, 2020.

[45] A. Zeb, A. Atangana, Z. A. Khan, and S. Djillali. A robust study of a piecewise fractional order covid-19 mathematical model. *Alexandria Engineering Journal*, 61(7):5649–5665, 2022.

[46] Y. Zhang, X. Yu, H. Sun, G. R. Tick, W. Wei, and B. Jin. Applicability of time fractional derivative models for simulating the dynamics and mitigation scenarios of covid-19. *Chaos, Solitons Fractals*, 138:109959, 2020.

[47] S. Zhao, Q. Lin, J. Ran, S. S. Musa, G. Yang, W. Wang, Y. Lou, D. Gao, L. Yang, D. He, and M. H. Wang. Preliminary estimation of the basic reproduction number of novel coronavirus (2019-ncov) in china, from 2019 to 2020: A data-driven analysis in the early phase of the outbreak. *International Journal of Infectious Diseases*, 92:214–217, 2020.

[48] Y. Zhou. *Basic Theory of Fractional Differential Equations*. World Scientific, Singapore, 2010.